BOREHOLD DEPLOYMENT OF BROADBAND QUARTZ TORSIONAL ACCELEROMETERS

Barry Block, et al

DIAX Corporation

Prepared for:

Air Force Office of Scientific Research
Advanced Research Projects Agency

30 November 1972

DIAX

Borehole deployment of broad-band quartz torsional accelerometers, Final report, 30 November 1972

prepared for

AIR FORCE OFFICE OF SCIENTIFIC RESEARCH

ARLINGTON, VIRGINIA

sponsored by

ADVANCED RESEARCH PROJECT AGENCY

ARPA ORDER NO. 2183

UNCLASSIFIED
Security Classification

DOCUMENT CONTROL DATA - R & D

(Security classification of title, body of abstract and indexing annotation must be entered when the overall report is classified)

1. ORIGINATING ACTIVITY *(Corporate author)*

DIAX Corporation
7825 Ivanhoe Avenue, Suite #202
La Jolla, California 92037

2a. REPORT SECURITY CLASSIFICATION
UNCLASSIFIED

2b. GROUP

3. REPORT TITLE

"Borehole Deployment of Broadband Quartz Torsional Accelerometers"

4. DESCRIPTIVE NOTES *(Type of report and inclusive dates)*
Scientific Final 17 April, 1972 to 30 November, 1972

5. AUTHOR(S) *(First name, middle initial, last name)*

Barry Block, Bruce Bartholomew, Jay Dratler, Jr., and Crispin Hollinshead

6. REPORT DATE	7a. TOTAL NO. OF PAGES	7b. NO. OF REFS
30 November 1972	64	

8a. CONTRACT OR GRANT NO.	9a. ORIGINATOR'S REPORT NUMBER(S)
F44620-72-C-0087	
b. PROJECT NO. Program Code No. 2F10	
c. ARPA Order No. 2183	9b. OTHER REPORT NO(S) *(Any other numbers that may be assigned this report)*
d.	

10. DISTRIBUTION STATEMENT

Approved for public release: distribution unlimited

11. SUPPLEMENTARY NOTES	12. SPONSORING MILITARY ACTIVITY
	Air Force Office of Scientific Research 1400 Wilson Boulevard Arlington, Virginia 22209

13. ABSTRACT

The DIAX torsional accelerometrers have been repackaged for borehole use. These broadband accelerometers have been described previously (Technical Report ARPA Contract F44620-72-C-0087). This final report will describe the borehole packaged system as it has been designed during the Feasibility Study Contract F44620-72-C-0087.

The basic sonde system is presently designed to operate at a pressure equivalent to a depth of 3000 feet of water.

It should be noted that the DIAX accelerometers provide true broadband information which extends from zero frequency to several Hertz. This enables the following phenomena to be investigated with a single system at no additional cost: 1) High frequency seismic signals (6 to 0.1 seconds period); 2) Low frequency seismic signals (60 to 6 seconds period); 3) Earth normal mode excitations (3600 to 60 seconds period); 4) Tectonic phenomena at nearly zero frequency.

The DIAX system is the only system with low noise, low drift and high sensitivity over this entire bandwidth. Operation at depth will allow isolation from surface noise sources yielding excellent quality data independent of local surface weather conditions.

DD FORM 1 NOV 68 1473

UNCLASSIFIED
Security Classification

14. KEY WORDS	LINK A		LINK B		LINK C	
	ROLE	WT	ROLE	WT	ROLE	WT
Accelerometers						
Seismometers						
Deep Hole Tiltmeter						
Borehole Tiltmeter						
Borehole Seismometer						
Tilt Sensor						
Gravity Meter						
Gravimeter						
Earth Strain and Tilt/Measurement						
Uplift Associated with Fluid Injection						
Tectonic Tilt						
Oil-Well Instrumentation						
Deep Hole Electronics						
Borehole Electronics						

FINAL REPORT

17 April 1972 through 30 November 1972

BOREHOLE DEPLOYMENT OF BROADBAND QUARTZ TORSIONAL ACCELEROMETERS

Sponsored by

Advanced Research Projects Agency

ARPA Order No. 2183

DIAX Corporation

Identification

Project Title:	Borehole Deployment of Broadband Quartz Torsional Accelerometers
ARPA Order No:	2183
Program Code No:	2F10
Name of Contractor:	DIAX Corporation
Contract Expiration Date:	30 November 1972
Amount of Contract:	$102,322
Contract No:	F44620-72-C-0087
Principal Invesitgator:	Barry Block
Telephone No:	(714) 459-4146

Table of Contents

Summary

The DIAX torsional accelerometers have been repackaged for borehole use. These broadband accelerometers have been described previously (Technical Report ARPA Contract F44620-72-C-0087). This final report will describe the borehole packaged system as it has been designed during the Feasibility Study Contract F44620-72-C-0087.

The basic sonde system is presently designed to operate at a pressure equivalent to a depth of 3000 feet of water.

It should be noted that the DIAX accelerometers provide true broadband information which extends from zero frequency to several Hertz. This enables the following phenomena to be investigated with a single system at no additional cost:

1) High frequency seismic signals
   (6 to 0.1 seconds period)
2) Low frequency seismic signals
   (60 to 6 seconds period)
3) Earth normal mode excitations
   (3600 to 60 seconds period)
4) Tectonic phenomena at nearly zero frequency

The DIAX system is the only system with low noise, low drift and high sensitivity over this entire bandwidth. Operation at depth will allow isolation from surface noise sources yielding excellent quality data independent of local surface weather conditions.

Introduction

The DIAX torsional accelerometers have been repackaged for borehole use. These broadband accelerometers have been described previously (Technical Report ARPA Contract F44620-72-C-0087). This final report will describe the borehole packaged system as it has been designed during the Feasibility Study Contract F44620-72-C-0087.

It should be noted that the DIAX accelerometers provide true broadband information which extends from zero frequency to several Hertz. This enables the following phenomena to be investigated with a single system at no additional cost:

1) High frequency seismic signals
   (6 to 0.1 seconds period)
2) Low frequency seismic signals
   (60 to 6 seconds period)
3) Earth normal mode excitations
   (3600 to 60 seconds period)
4) Tectonic phenomena at nearly zero frequency

The DIAX system is the only system with low noise, low drift and high sensitivity over this entire bandwidth. Operation at depth will allow isolation from surface noise sources yielding excellent quality data independent of local surface weather conditions.

The basic sonde system is presently designed to operate at a pressure equivalent to a depth of 3000 feet of water. Operation at greater depths

is possible by modifying the "O" ring seals and increasing the sonde wall thickness. The outer diamter of the sonde is 5 3/4 inches.

The sonde system is supplied with a controller at the surface which performs the following operations in a failsafe fashion:

1) Locking the sonde to the borehole casing
2) Releasing protective clamps and locks
3) Tilting each accelerometer up to ± 3° to compensate for borehole tilt
4) Calibrating each accelerometer with respect to the local gravity field
5) Determining relative frequency calibration of each accelerometer from zero frequency to several Hertz.
6) Adjusting the mechanical zero of the vertical accelerometer
7) Monitoring environmental conditions in the sonde.

The sonde controller contains a pair of digital data transceivers capable of kilobaud transmission rates, which can function as the nucleus of a downhole digital transmission system.

Protective devices are incorporated into the borehole lock and cable-head to insure retrieval if the lock fails to release.

The electronic sensing system for each axis operates by phase-sensitive detection which is an optimal signal-to-noise detection method.

The system is built in a modular fashion so that elements may be substituted in the sonde with ease. The modules as listed from bottom to top are:

1) Centralizer
2) Vertical Accelerometer Module
3) Horizontal Accelerometer N-S Module
4) Horizontal Accelerometer E-W Module
5) Borehole Lock
6) Cable Entry
7) Cable
8) Surface Control System

The Final Report is divided into three sections:

I. Sonde Mechanical Assembly
II. Electronics
III. Noise Tests

Each section covers in detail the corresponding material.

I. Sonde Mechanical Assembly

Borehole deployment of the DIAX broadband accelerometers requires a repackaging for operation in the hostile borehole environment. The borehole package is designed to fit down standard 6 inch I.D. casing pipe. The instruments must be protected from the shocks expected during deployment of the package and handling at the borehole site. Since these instruments need to be leveled for operation, a tilt platform is required with sufficient dynamic range to allow for borehole inclinations, as well as being sensitive enough to perform tilt calibrations after deployment. The physical vessel, or sonde, is required to withstand operation beneath 2000 feet of water while maintaining its integrity as a support structure for the accelerometers and attendant electronics. The instruments must be aligned so that the two horizontal accelerometers are perpendicular to each other and to the sensitive axis of the vertical accelerometer. Finally, the sonde must be anchored to the borehole casing in a manner which is reversible in operation, secure when locked, and retrievable in case of failure. These requirements set the boundary conditions of our design. The accelerometer designs are treated in detail in the Technical Report to this contract.

The sonde has an outer diameter of 5 3/4" with 1/4" wall thickness. The design is sectional to facilitate manufacture and assembly. The

sections consist of lengths of casing and threaded collars. The joint between casing and collar is sealed with an "O" ring, rated at 1500 PSI. The casing is internally threaded and acts as a spacer/carrier for the collars, which support the actual accelerometers. The tilt calibrator is assembled on the collar, providing a steady base for the instrument. The three instruments are located one above the other in the sonde, with the vertical accelerometer at the bottom. This is the least tilt sensitive, so it is placed furthest from the hole lock (see Figure I-1).

The tilt calibrator modules are basically three motor-driven micrometers, two hold-down springs and a support structure. The micrometers are heavy duty (5/16" spindle) Starrett brand driven through gears and idlers by three stepping motors. The steppers are 15°/step Rapid-Syn motors made by Computer Devices Corp. The motors have a 3600:1 gearhead on the output. This ratio was chosen so that one step gives a tilt angle of 10^{-7} rad. This resolution is required to allow a meaningful calibration using tilt. The advantage of stepping motors is that their speed can be ranged from one step at a time to 1000 rpm. The higher speeds are used in the initial leveling which may involve several degrees of tilt to compensate for tilt of the borehole. Due to the physical size of the instrument vacuum can and the I.D. of the sonde, the total tilt range is less than $\pm$ 3°. Therefore, the borehole must be specified to be vertical to within 3° for operation. Each motor drives a length of pinion wire which, in turn, drives a gear on one micrometer. This arrangement allows for the vertical motion of the micrometer gear as the spindle is run in and out (see Figure I-2).

Block Diagram of SONDE

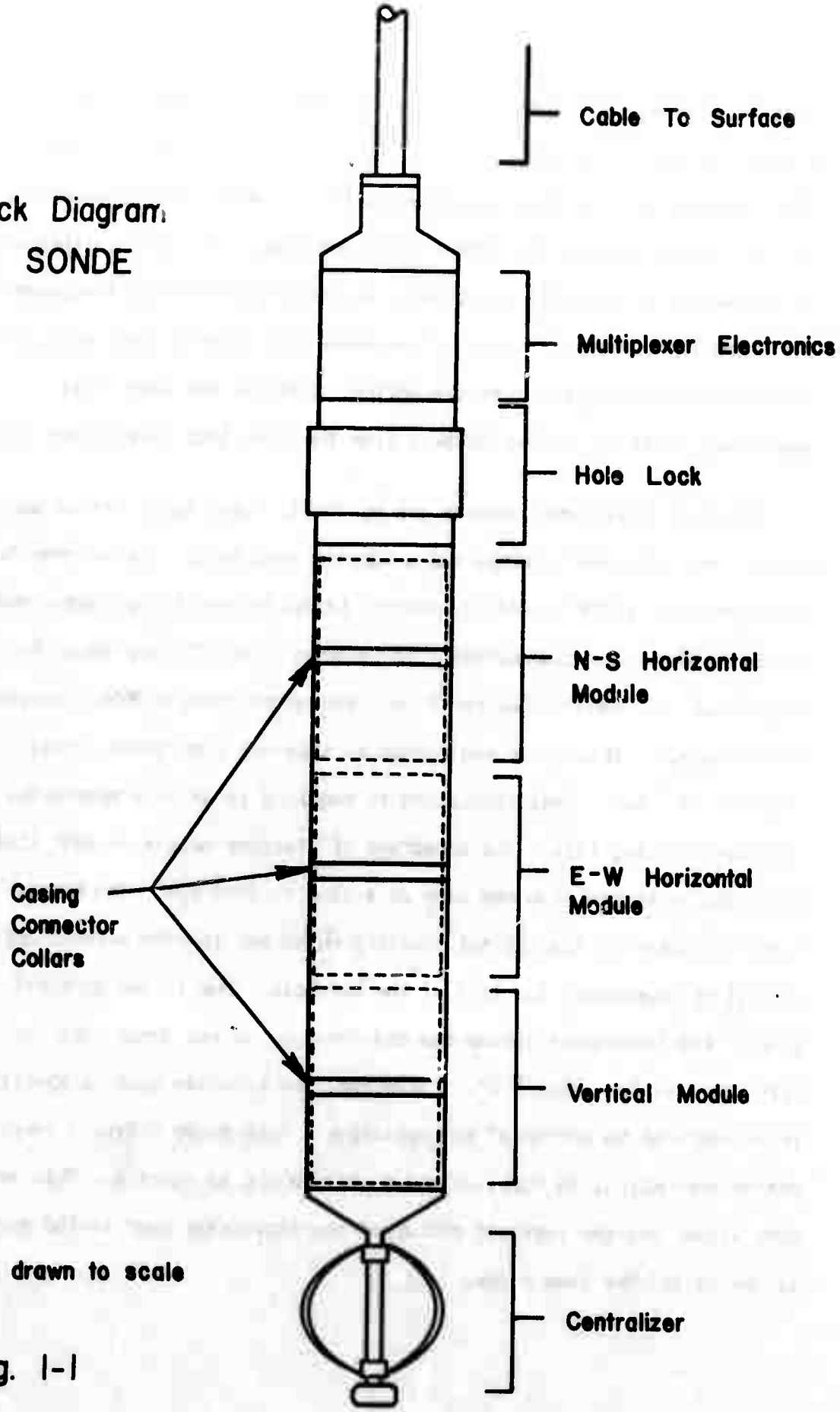

not drawn to scale

Fig. 1-1

Cutaway of a Calibrator Assembly

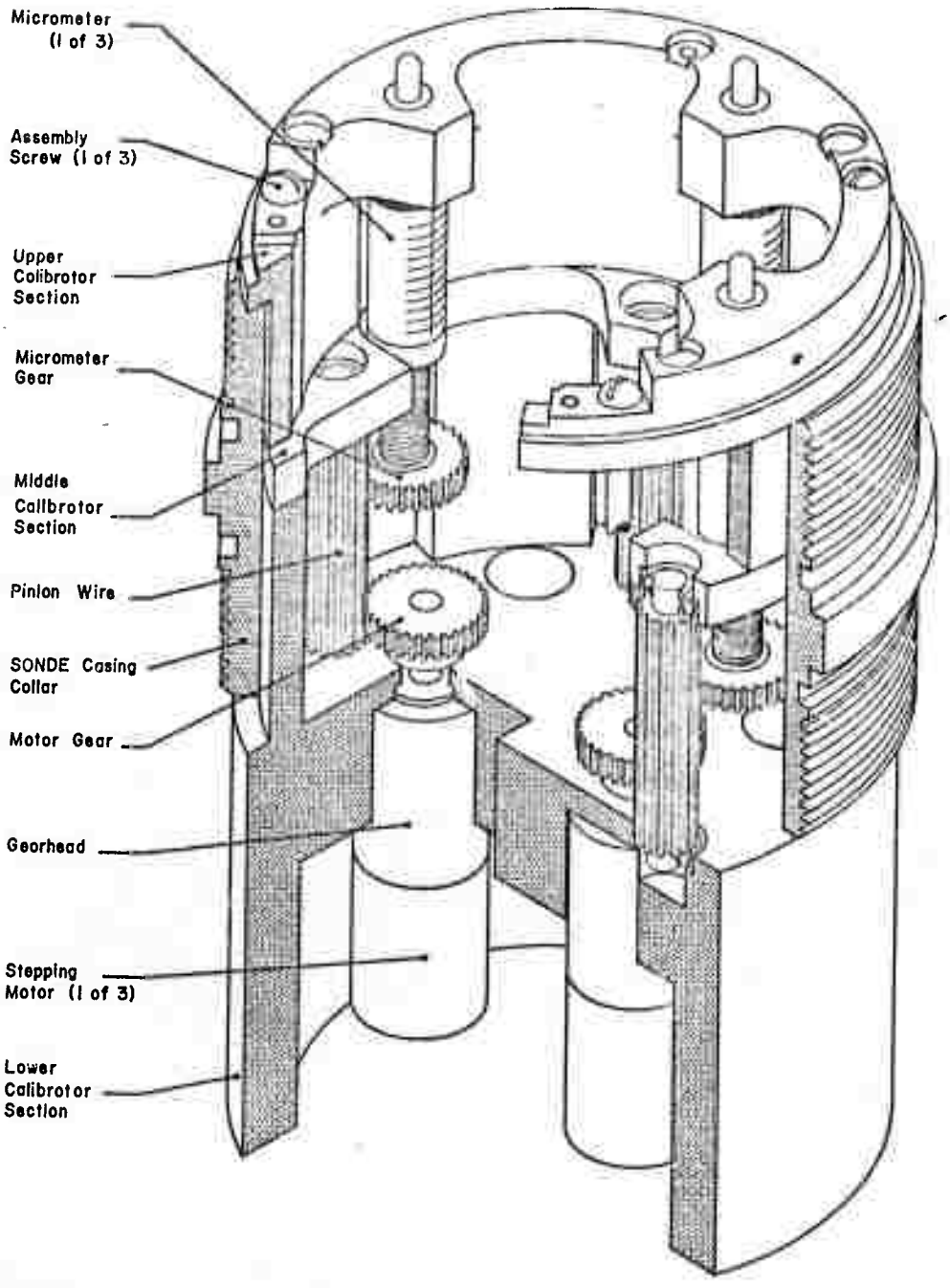

Fig. 1-2

Detail of Horizontal Module (less electronics)

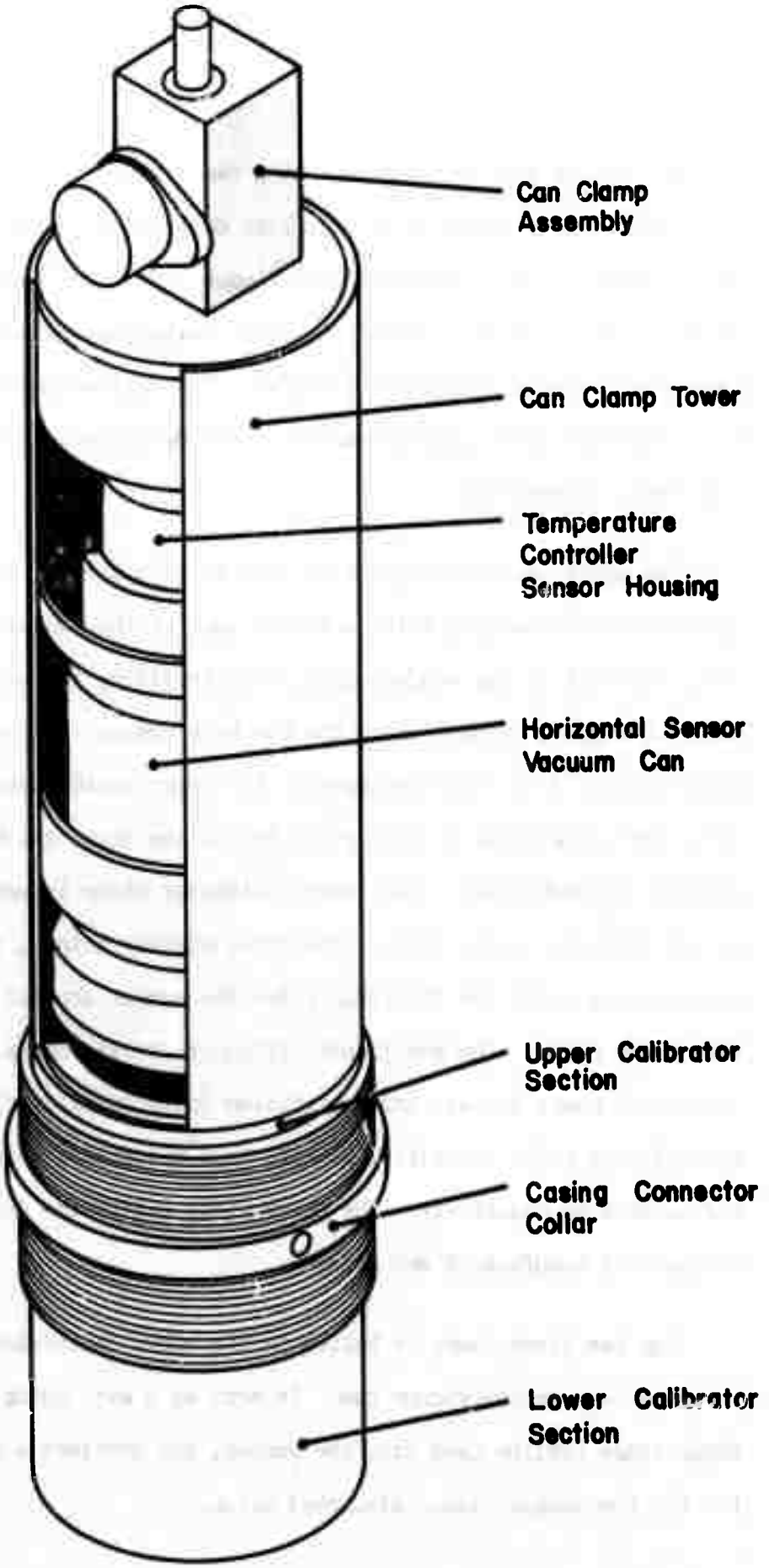

Fig. 1-3

The module assembly consists of a can clamp tower, a three piece calibrator, and a sonde collar which is constrained between the upper and lower pieces of the calibrator (see Figure I-3). The sonde collar can rotate relative to the calibrator until the calibrator assembly is tightened, rigidly clamping the collar. This allows the sonde collar to be threaded onto a casing section while maintaining a specific calibrator orientation.

The upper calibrator piece is made of 4340 steel (high strength) and carries the micrometers which actually support the sensor. This piece rests directly on the sonde collar, thus providing the most direct, i.e., the most stable, connection to the borehole casing. The middle calibrator piece is also 4340 steel and carries the upper pinion wire bearings. Three 1/8" dowel pins in this piece locate the three calibrator pieces relative to each other. The lower calibrator piece is made of aluminum, for its thermal conductivity. The three stepper motors, the lower pinion wire bearings, and the electronics for the sensor are all supported from this lower piece. The electronics (stepper driver boards, temperature controller power driver, and a precision drive oscillator) are therefore located near their respective sensor, thus minimizing inter-sonde cabling and maximizing modularity. The three piece calibrator design is necessary for ease of manufacture and assembly.

The can clamp tower is bolted to the upper calibrator piece and surrounds the sensor vacuum can. It acts as a wire guide which holds the inter-sonde cabling away from the sensor, and provides a mounting platform for the top sensor clamp, discussed below.

In order to maximize the tilt lever arms, the micrometer triangle hypotenuse is along the diameter of the can. To eliminate the possibility of the can falling over as a result of tilting too far, two hold-down springs are used. These springs provide a total force of 20 pounds. One end of each is anchored to the lid of the can, and the other end is anchored in the calibrator structure. Since the lid of the can is electrically at signal ground and the sonde is at panel ground, the lid end of the springs are electrically isolated from the lid by the use of mica insulators.

The support micrometers are insulated for the same reason. The spindles of the micrometer are ball-ended and ride in three kinematic mounts (three balls, two rods, and one flat) which uniquely position the lid relative to the calibrator at the same time allowing for thermal expansion. These kinematic mounts are electrically insulated from the lid using mica insulator sheets. This method has been used previously on these types of accelerometers with excellent results both mechanically and electrically.

During transportation and deployment of the sonde, it is necessary to secure the instrument to protect against impacts due to handling. This is accomplished in two ways. First the inertial mass of each accelerometer is clamped by a compliant member. This clamp is driven directly by a motor on the horizontal instruments, while on the vertical instrument the clamping is done by driving the plate assembly against an internal stop, using the zero adjust mechanism. The second protective method consists

of mechanically isolating the vacuum can from the sonde. The three micrometers on each tilt calibrator platform are withdrawn to the end of their range. The hold-down springs pull the vacuum can down onto four rubber bushings which support the can beyond the ends of the retracted micrometers. The four small bushings rest in recesses in the calibrator, which provide lateral orientation and insure that the micrometers will reseat in the kinetic mounts when re-projected. A large rubber bushing is driven down from above the can, clamping the instrument firmly, but not rigidly, thus providing a measure of shock isolation. This upper clamp is motor driven, through a worm gear, so pressure can be maintained after the motor is shut off. The drive mechanism is mounted on the can clamp tower discussed above.

The problem of clamping the entire sonde into the borehole was solved by adapting a proven borehole clamp. The Geotech expanding ring clamp was designed to fit our sonde package. This unit is driven by a geared D.C. motor (the same motor as in the Geotech design) which screws two wedges together, thus forcing a split ring to expand against the hole casing. The process is entirely reversible, yet provides excellent clamping when set. Should the motor fail to release, a weak link allows the clamp to be selectively broken to retrieve the sonde. For stability, the borehole clamp is located near the top of the sonde so that most of the weight hangs below the clamp.

The cable from the surface is anchored at the upper end of the sonde through a cablehead which will separate at the sonde (leaving the cable

intact) at a predetermined tension to allow for retrieval, with grappling apparatus, should the borehole clamp fail to release.

II. Electronics

Introduction

The electronic circuitry for the DIAX three-axis borehole accelerometer is divided into two separate systems. The first system contains those circuits which are required for operation of the three accelerometers and which must remain on during data acquisition. The three sets of transducer electronics and temperature controllers fall into this category. The second system consists of the sonde controller and its power supplies, including all circuits necessary for sonde deployment, instrument setup, leveling, calibration, and monitoring of instrument performance. The sonde controller is used during initial deployment and during routine testing and calibration, but is normally off when the accelerometers are left unattended to gather data.

The two electronics systems, accelerometer circuitry and the sonde controller, are entirely separate and independent. Each derives power from its own supply. For the accelerometer electronics, the power supply is a DC system containing batteries capable of delivering full power for 24 hours. With this battery back-up system, accelerometer performance is independent of local line irregularities and power failures less than 24 hours in duration. Power for the sonde controller, which is never operated unattended, is derived directly from the mains.

Accelerometer Electronics

A block diagram of the accelerometer electronics is shown in Fig. II-1. The entire system consists of seven subsystems; one power supply, three sets of transducer electronics, and three precision thermostats. Since the three accelerometers, one for each axis, are electrically identical, the three sets of transducer electronics are the same, as are the three thermostats. The circuits are shown individually in the figure to clarify grounding and power arrangements.

Each of the three accelerometers in the borehole system contains a differential capacitance position transducer to detect the displacement of its inertial element. The transducers are operated at high audio frequencies and the resulting signals are processed by preamplification and phase-sensitive detection. A stable drive oscillator provides the exciting signal, and a drive transformer with closely matched secondaries supplies ou -of-phase signals to the outer transducer plates. The preamplifier and phase-sensitive detector (lock-in amplifier) provide a DC output signal proportional to the displacement of the inertial element from null. In the DIAX system, these components are obtained from commercial manufacturers of electronic equipment, as shown in Table II-1. The custom-designed drive oscillator produces a sine wave of 0-10 V peak-to-peak amplitude with an amplitude stability of 0.01%/°C and 0.01% long term. The toroidal drive transformer has secondaries matched to better than 1 part to 10^4. The preamplifier is designed for lowest noise at the transducer operating frequency, having an equivalent input noise of 5 nV/$\sqrt{\text{Hz}}$ RMS with a 80 pf

ACCELEROMETER ELECTRONICS

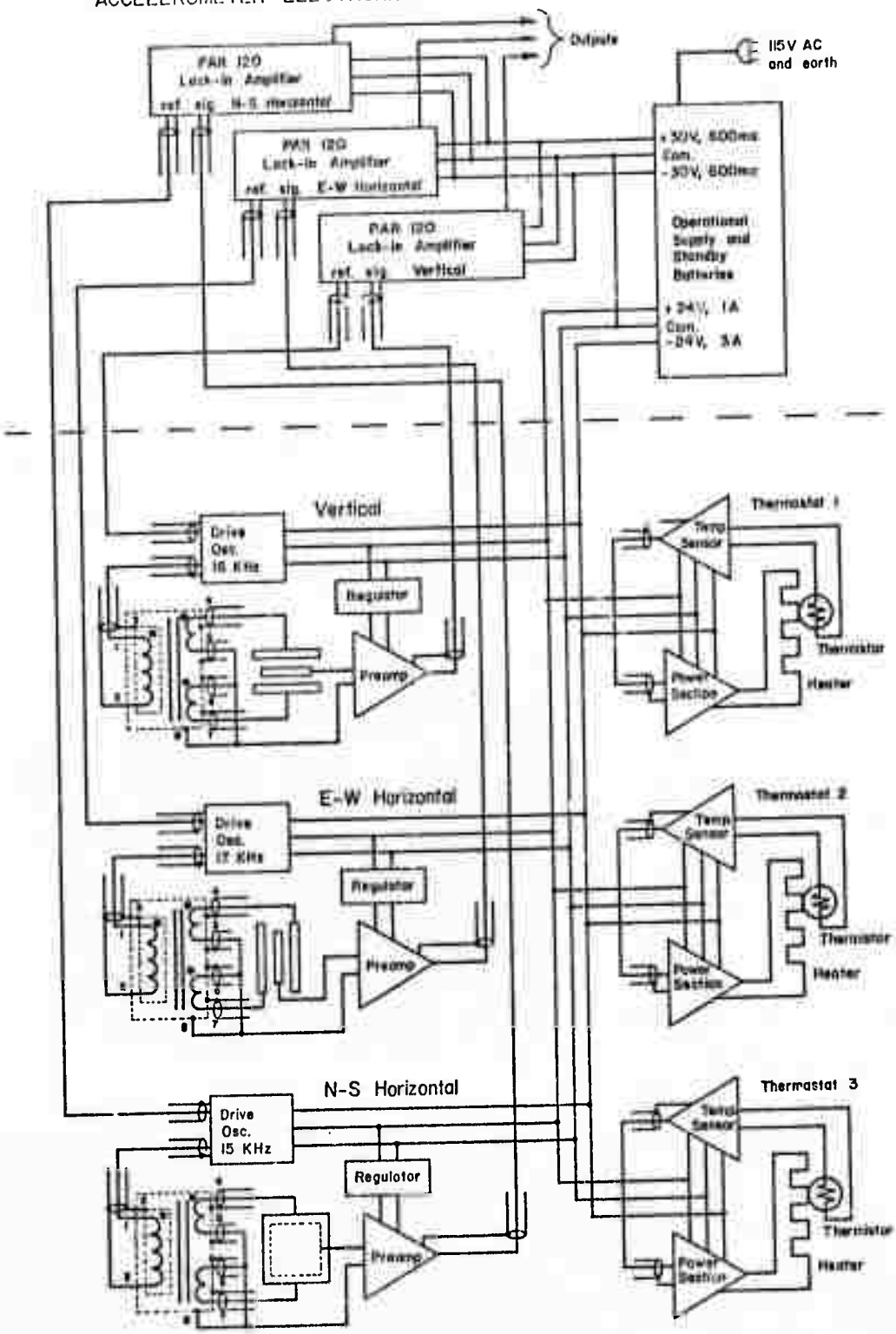

Fig. II-1

ACCELEROMETER ELECTRONICS

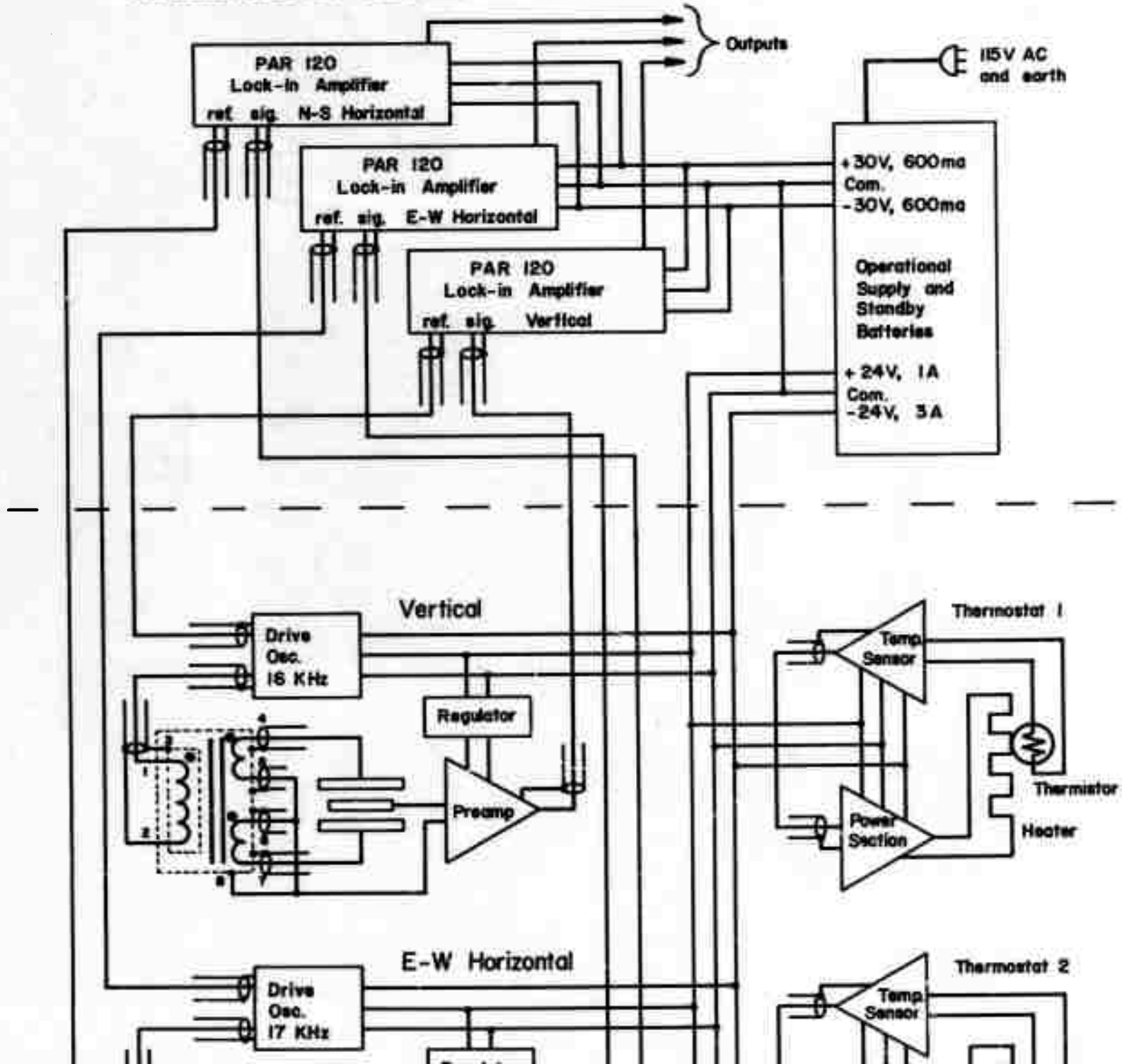

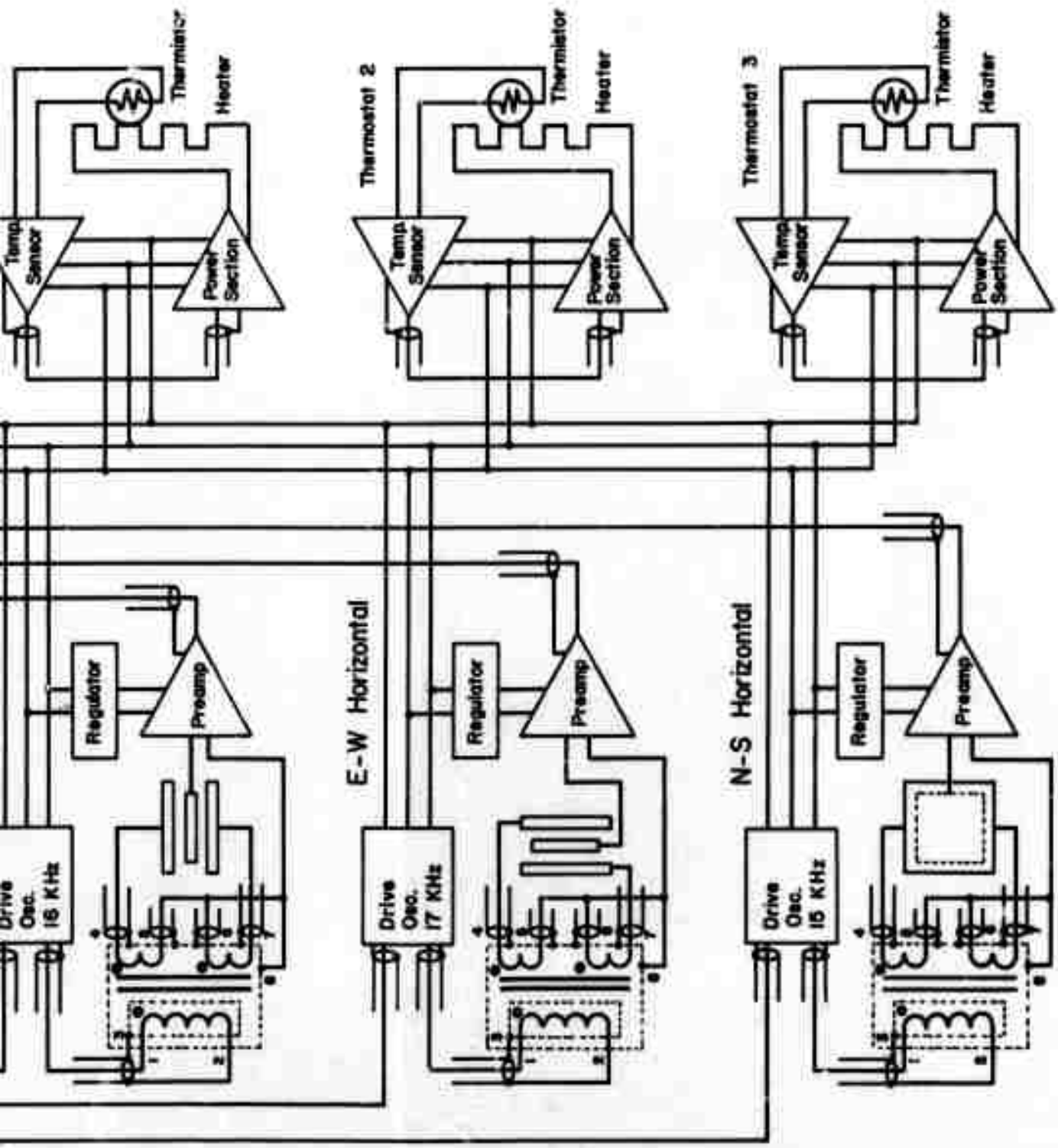
Thermistor
Heater
Temp. Sensor
Power Section
Thermostat 2
Thermistor
Heater
Temp. Sensor
Power Section
Thermostat 3
Thermistor
Heater
Temp. Sensor
Power Section
E-W Horizontal
Regulator
Preamp
Drive Osc. 16 KHz
Regulator
Preamp
Drive Osc. 17 KHz
N-S Horizontal
Regulator
Preamp
Drive Osc. 15 KHz

Fig. II-1

capacitative source termination (see section on Noise below). The lock-in amplifier used here is the least expensive readily available commercial instrument with sufficiently low input noise to allow the preamplifier noise to dominate. Use of these OEM items is dictated by the stringent noise and stability requirements.

The frequency of operation of the accelerometer transducers is dictated by noise characteristics of the preamplifier (see section on Noise below). Measurements have shown that with a capacitative source of 80 pf, the input noise of the best available preamplifiers is lowest at frequencies between 10 and 20 kHz, attaining a minimum at about 16 kHz (see Figure III-6 below). For this reason the most sensitive instrument, the vertical, is run at exactly 16 kHz, while the two horizontals are run at neighboring frequencies. The frequencies of operation of the three instruments are kept quite distinct to avoid any possibility of crosstalk.

The cabling and grounding arrangements for the transducer circuitry are shown in detail in Figure II-1. It should be emphasized that the configuration shown here has been designed as conservatively as possible. Each transducer signal is conveyed to the surface on a separate coaxial cable, whose shield serves as the corresponding signal ground. The three reference signals from the drive oscillators are brought to the surface on separate coaxial lines to minimize crosstalk.

In practice, it may be possible to combine all the signal lines into one coaxial cable since the signal grounds carry little current.

The three lock-in amplifiers at the surface may suffice to separate the distinct frequencies without crosstalk. It may also be possible to combine the reference lines by using additional crystal filters at the surface. This would result in a saving of four coaxial lines in the main cable. However, to determine whether this is possible, actual in situ tests must be made with a ragline cable, as theoretical models of crosstalk are never satisfactory.

Owing to the temperature coefficient of elasticity of the quartz fibers used in the accelerometers, strict temperature regulation of the mechanical systems is necessary. Each accelerometer has its own precision proportional thermostat, as shown in Fig. II-1. The thermostats are of in-house designs, being improved and miniaturized versions of the thermostats successfully used for the laboratory accelerometers.

A schematic diagram of one of the thermostats is shown in Fig. II-2. The temperature of the accelerometer's vacuum housing is sensed by a thermistor in series with a standard resistance,which together divide the output of a precision voltage source. The divider signal, which is null when the two resistances are equal, is amplified by a high-gain chopper stabilized operational amplifier (AD234X) at full open loop gain. This part of the thermostat, called the temperature sensor, produces an error signal whose full range of ± 10 V corresponds at DC to ± 33 microdegrees centigrade change in the thermistor. The error signal is amplified by a one-sided power section, which supplies current to a heater wound around the vacuum enclosure. The power section contains a hybrid

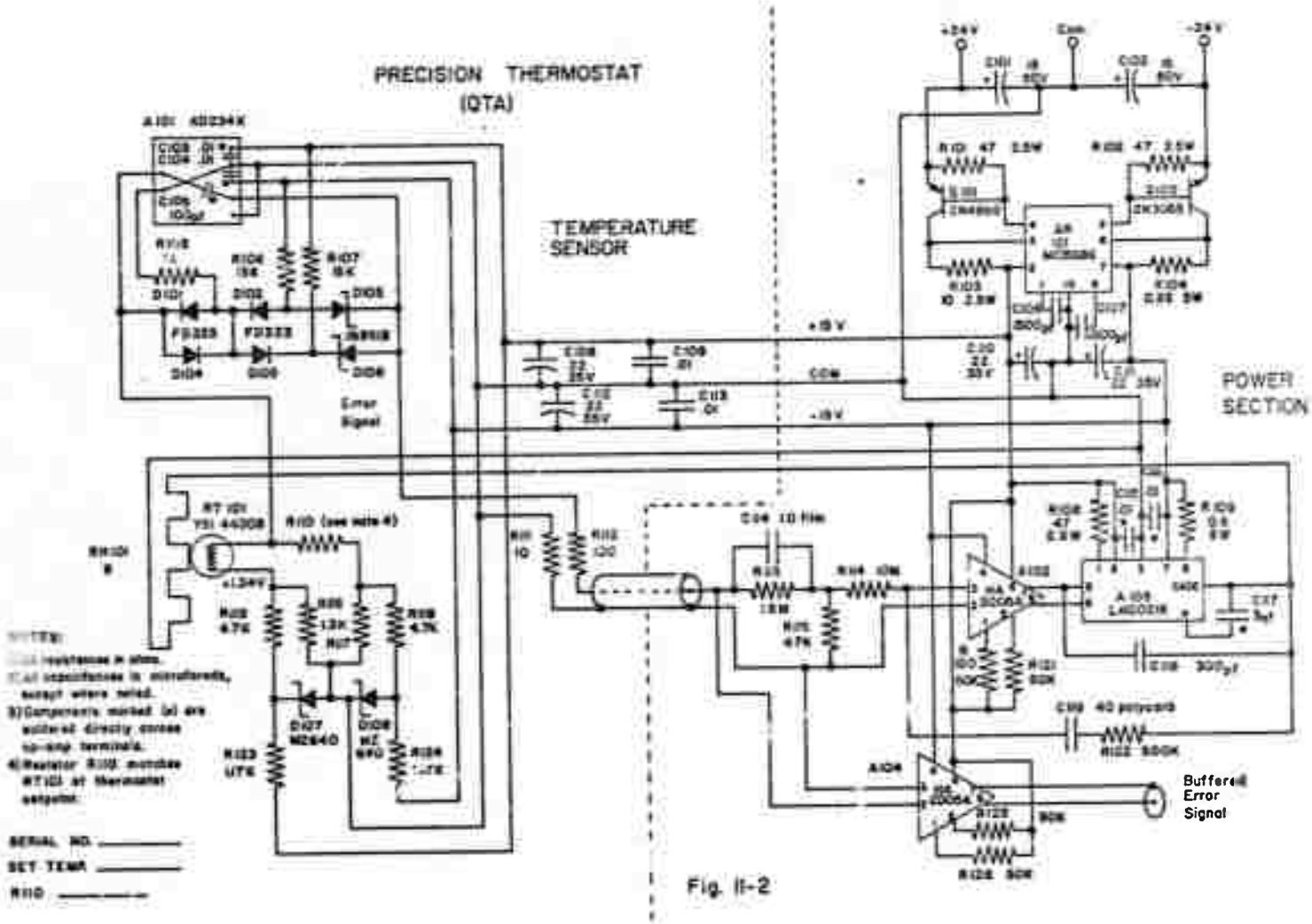
PRECISION THERMOSTAT
(QTA)
TEMPERATURE SENSOR
POWER SECTION
Error Signal
Buffered Error Signal
+15V
COM
-15V
SERIAL NO. _____
SET TEMP _____
R110 _____

Fig. II-2

PRECISION THERMOSTAT
(QTA)

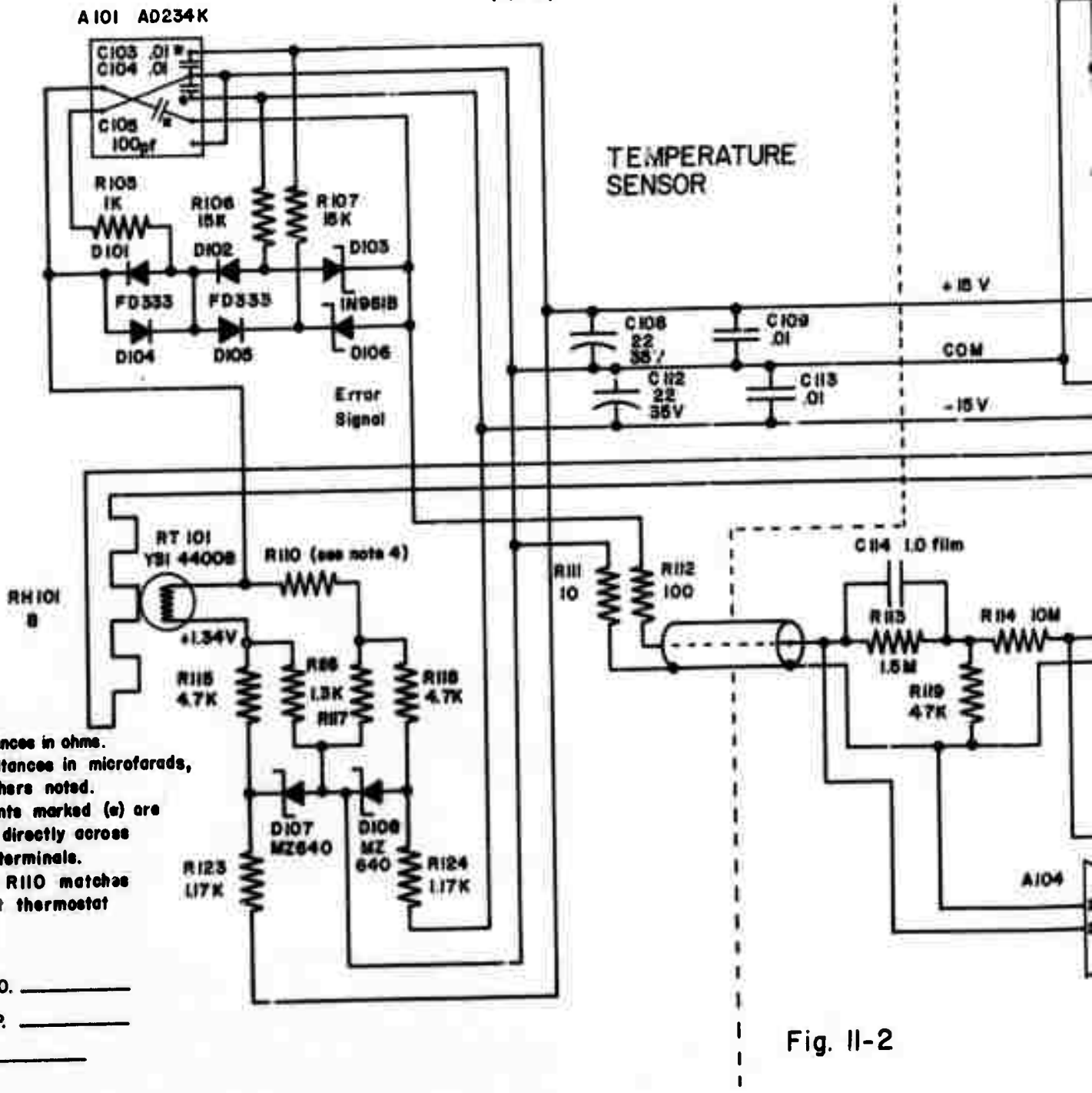

NOTES:

1) All resistances in ohms.
2) All capacitances in microfarads, except where noted.
3) Components marked (a) are soldered directly across op-amp terminals.
4) Resistor R110 matches RT101 at thermostat setpoint.

SERIAL NO. _____

SET TEMP. _____

R110 _____

Fig. II-2

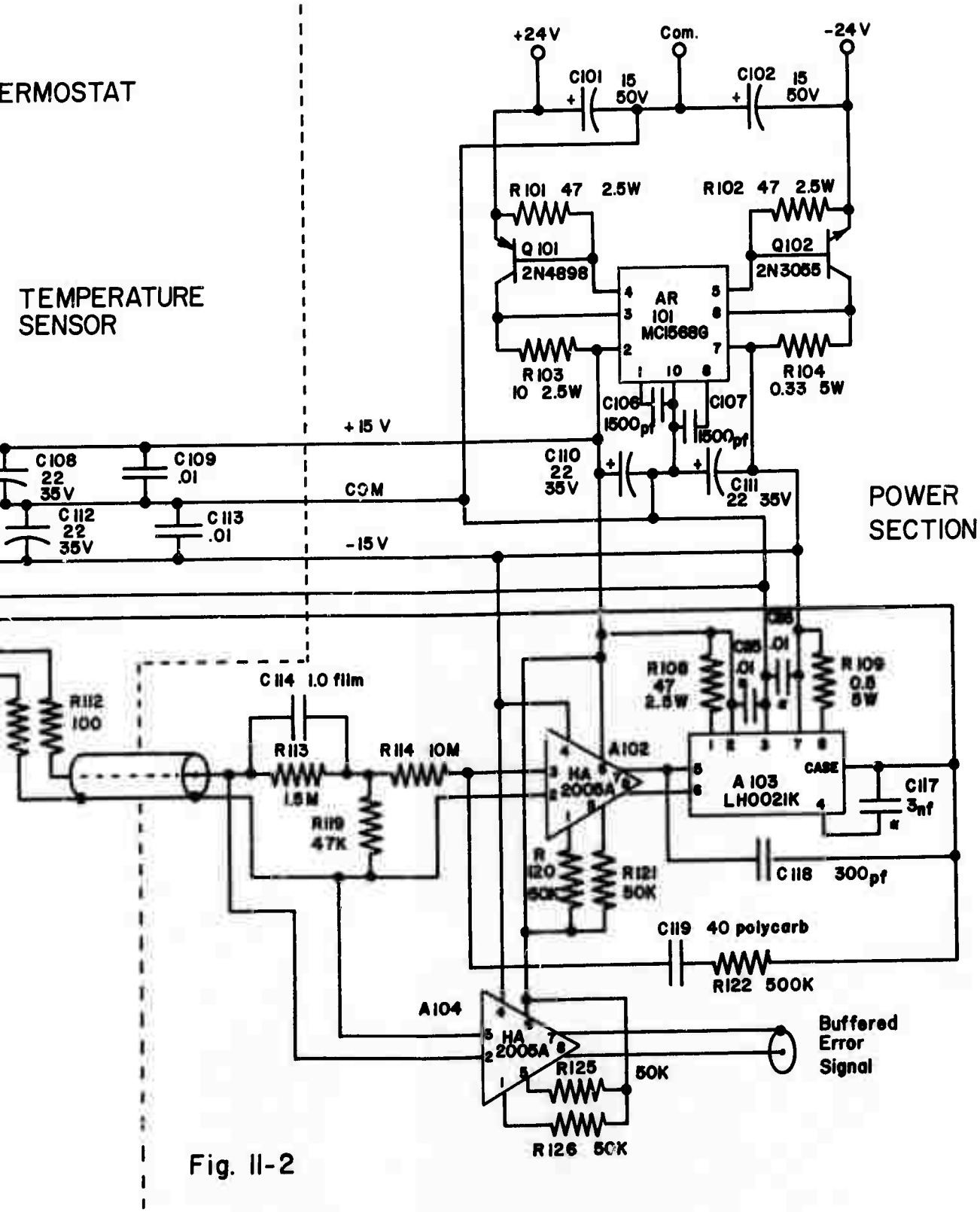
ERMOSTAT
TEMPERATURE SENSOR
+24V
Com.
-24V
C101 15 50V
C102 15 50V
R101 47 2.5W
R102 47 2.5W
Q101 2N4898
Q102 2N3055
AR 101 MC1568G
R103 10 2.5W
R104 0.33 5W
C106 1500pf
C107 1500pf
C110 22 35V
C111 22 35V
+15 V
COM
-15 V
C108 22 35V
C109 .01
C112 22 35V
C113 .01
POWER SECTION
R112 100
C114 1.0 film
R113 1.5M
R114 10M
R119 47K
A102 HA 2005A
R108 47 2.5W
C105 .01
C115 .01
R109 0.5 5W
A103 LH0021K
CASE
C117 3nf
C118 300pf
R120 50K
R121 50K
C119 40 polycarb
R122 500K
A104 HA 2005A
R125 50K
R126 50K
Buffered Error Signal

Fig. II-2

power operational amplifier with an input lead-lag network and an integrating feedback network to provide the proper phase response for stabilizing the entire loop.

The standard resistance is selected to determine a thermal null point about 5°C above the ambient temperature. Thus, there is always current in the heater winding, and small changes in this current compensate for variations in ambient temperature. The thermostat as a whole is a truly proportional system. In normal operation, the amplifier circuits are in the unsaturated mode.

The most critical parts of the thermostat are the thermal elements: the thermistor, heater, vacuum enclosure, and thermal insulation. Care is necessary in assembly of these components to insure that proper thermal contact is maintained. The heater is a 30-foot-long winding of nickel high resistance wire, bound to the vacuum enclosure surface with glyptal varnish cement. To avoid inductive effects on the instrument, the winding is bifilar. The thermistor is mounted directly on top of one loop of the heater winding with Wakefield Engineering Co. Delta Bond 152 thermally conducting epoxy.

In laboratory tests, this temperature regulator provides stable and proportional control with 1 1/2" of thermal insulation surrounding the vacuum enclosure while in the presence of ambient temperature variations of as much as 5°C in five hours. Heater current varies between 150 and 450 ma, depending upon the ambient temperature. In the sonde, the thermal

insulation must be reduced to 1/8" of foam due to space limitations. No problems in stabilizing the controller are anticipated, as ambient temperature variations in the borehole are expected to be about 10^{-3}°C peak-to-peak. It may be necessary, however, to alter the values of some of the components in the lead-lag network or feedback loop of the power section to stabilize the controller under borehole conditions. In the borehole, it may be possible to run the controller at a much smaller differential between regulated and ambient temperature. Thus final values of stabilizing components, standard resistance, and mean heater current will not be known until tests can be made with an actual section of the sonde.

One final word about the thermostats is in order. Experience with laboratory models operating in vaults has shown that strict temperature control is necessary for the DIAX vertical accelerometer. However, according to design calculations, the horizontal accelerometers are about 1000 times less sensitive to temperature than the vertical. In addition, temperature variations in the borehole are expected to be small. Thus, it may be possible to obtain good data without using thermostats for the horizontal accelerometers, though some regulation will probably be necessary for the vertical. As usual, a conservative philosophy has been adopted here in that temperature control for the horizontal instruments will be abandoned only when in situ tests prove that this is feasible. It is easy to turn the thermostats off, once they are installed, for a comparison test of their usefulness.

The accelerometer electronics, consisting of the three sets of transducer electronics and the three thermostats, operates from two dual DC power supplies with battery back-up. Downhole components are supplied from ± 24 volt lines, while + 30 V is required at the surface for the PAR Model 120 lock-in amplifiers.

Estimated current requirements are given in Table II-2. Of these values, those for the drive oscillator current drain and heater current are based on design parameters, and are likely to be over-estimates. Exact values will be determined during final testing. Battery back-up for the accelerometer electronics system is designed to provide the currents given in Table II-2 for a 24-hour period in the event of power failure.

Sonde Controller

The sonde controller, a block diagram of which is shown in Figure II-3, is used for deployment, set-up, calibration, and instrument evaluation. Its main function is the remote control of the various motors and auxiliary sensors in the sonde. As discussed in the section on mechanical design, there are two DC motors and three stepping motors associated with each of the three accelerometers. The two DC motors drive the vacuum housing clamp and the mass lock, which protect the sensitive components of the accelerometers during deployment. (In the vertical instrument, the mass lock and mechanical zero adjustment are controlled by the same motor.) The three stepping motors drive precision micrometers through reduction gears for tilting and calibration. During initial set-up, the three stepping motors for each accelerometer are run in tandem to lift the vacuum enclosure off of its protective pad. There is also a large DC motor which drives the borehole casing clamp.

As for auxiliary sensors, the sonde controller contains a switching device to minimize the number of cable conductors needed for routine monitoring and calibration. Signals to or from a given one of the several auxiliary devices may be routed through a single coaxial cable. Analog signals to be monitored are the three buffered error signals from the thermostats and signals from monitors of temperature and pressure, which may be installed in the sonde. Other switching channels

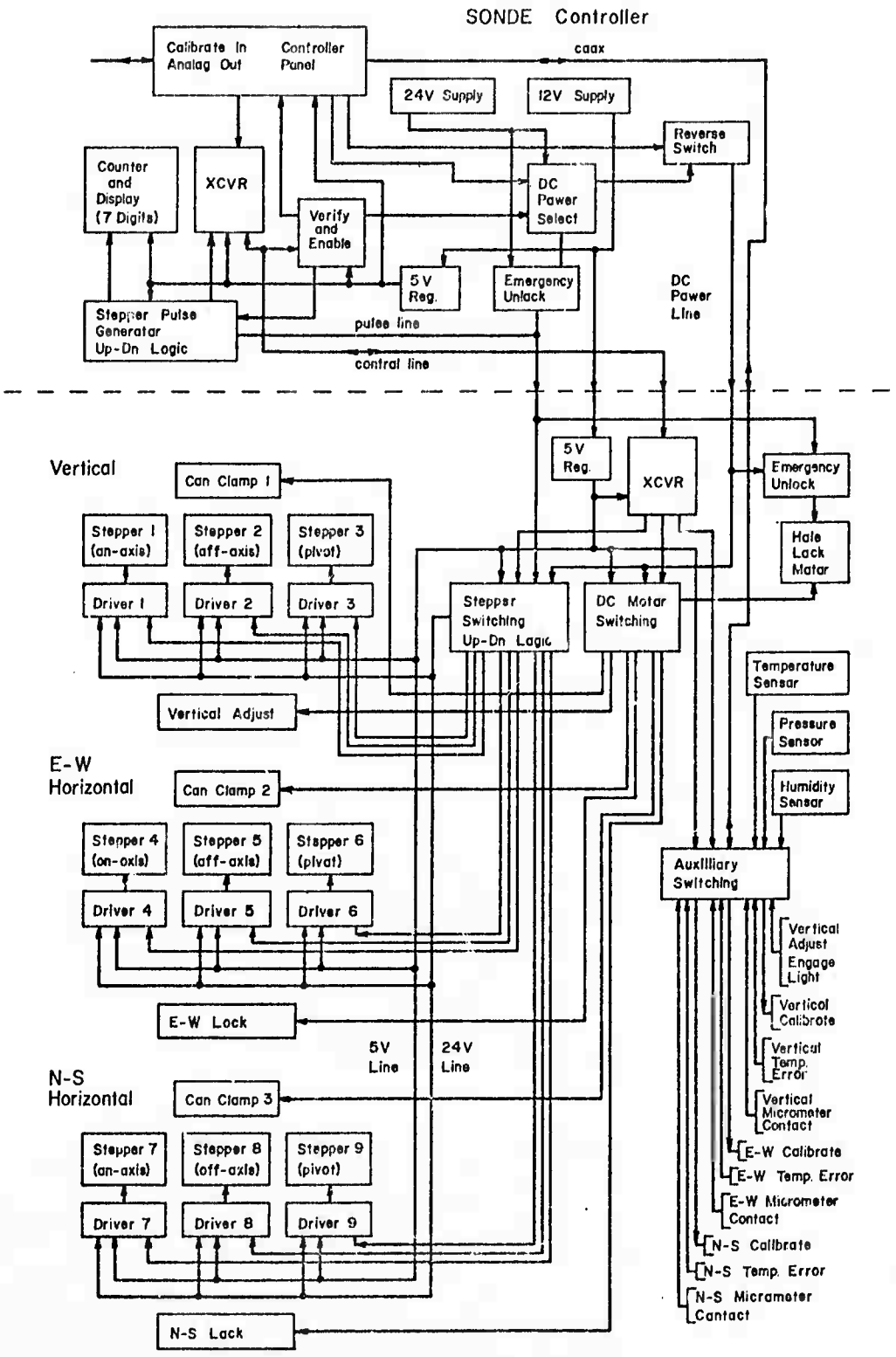
SONDE Controller
Calibrate In Analag Out
Controller Panel
caax
24V Supply
12V Supply
Reverse Switch
Counter and Display (7 Digits)
XCVR
Verify and Enable
DC Power Select
5V Reg.
Emergency Unlock
DC Power Line
Stepper Pulse Generatar Up-Dn Logic
pulse line
contral line
Vertical
Can Clamp 1
Stepper 1 (an-axis)
Stepper 2 (aff-axis)
Stepper 3 (pivot)
Driver 1
Driver 2
Driver 3
Stepper Switching Up-Dn Logic
DC Motar Switching
Vertical Adjust
E-W Horizontal
Can Clamp 2
Stepper 4 (on-axis)
Stepper 5 (aff-axis)
Stepper 6 (pivat)
Driver 4
Driver 5
Driver 6
E-W Lock
5V Line
24V Line
N-S Horizontal
Can Clamp 3
Stepper 7 (an-axis)
Stepper 8 (off-axis)
Stepper 9 (pivot)
Driver 7
Driver 8
Driver 9
N-S Lock
5V Reg.
XCVR
Emergency Unlock
Hole Lock Motar
Temperature Sensar
Pressure Sensor
Humidity Sensar
Auxilliary Switching
Vertical Adjust Engage Light
Vertical Calibrate
Vertical Temp. Error
Vertical Micrometer Contact
E-W Calibrate
E-W Temp. Error
E-W Micrometer Contact
N-S Calibrate
N-S Temp. Error
N-S Micrometer Contact

Fig. II-3

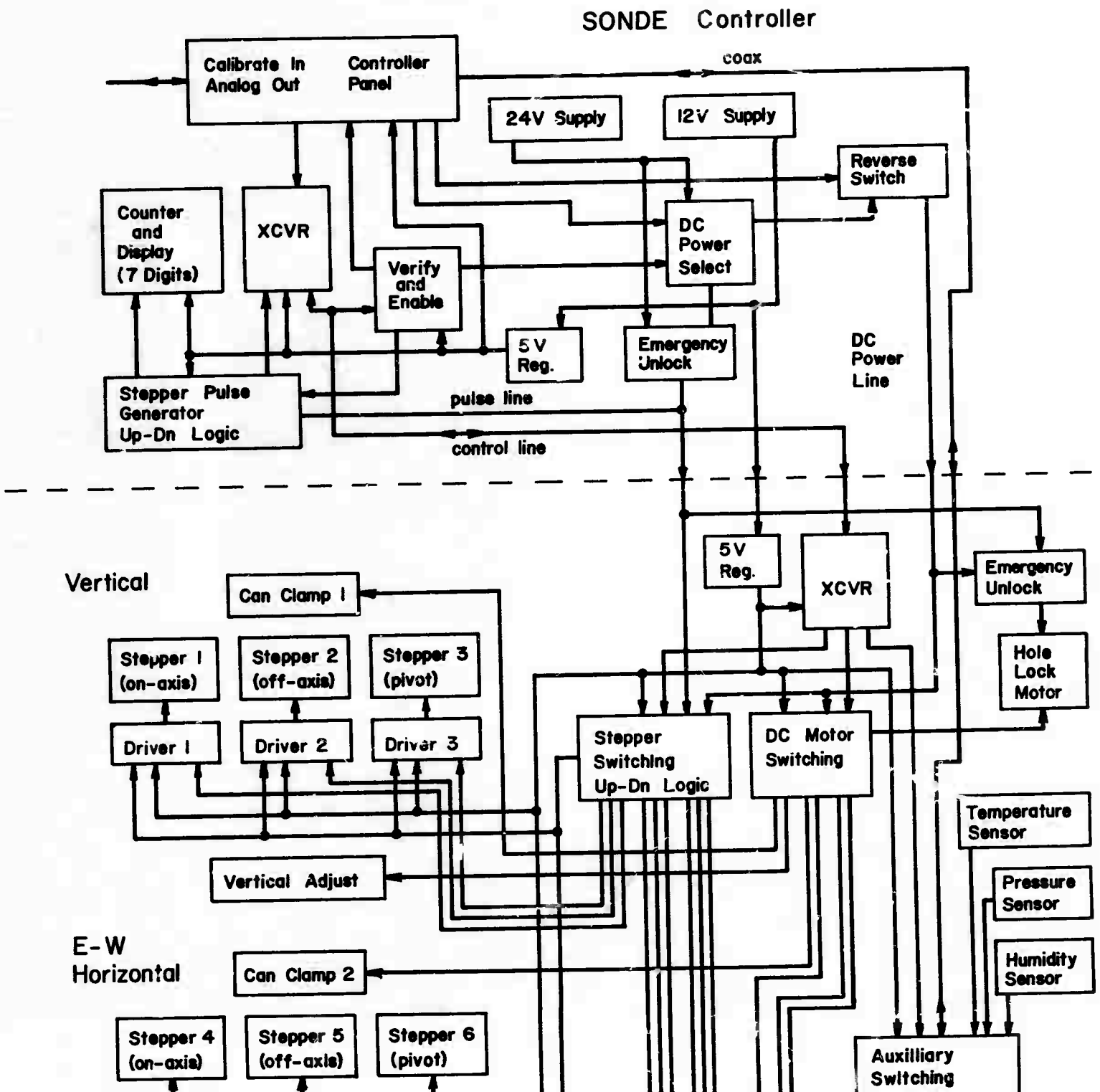
SONDE Controller
Calibrate In
Analog Out
Controller
Panel
coax
24V Supply
12V Supply
Reverse
Switch
Counter
and
Display
(7 Digits)
XCVR
Verify
and
Enable
DC
Power
Select
5V
Reg.
Emergency
Unlock
DC
Power
Line
Stepper Pulse
Generator
Up-Dn Logic
pulse line
control line
5V
Reg.
XCVR
Emergency
Unlock
Vertical
Can Clamp 1
Stepper 1
(on-axis)
Stepper 2
(off-axis)
Stepper 3
(pivot)
Hole
Lock
Motor
Driver 1
Driver 2
Driver 3
Stepper
Switching
Up-Dn Logic
DC Motor
Switching
Temperature
Sensor
Vertical Adjust
Pressure
Sensor
E-W
Horizontal
Can Clamp 2
Humidity
Sensor
Stepper 4
(on-axis)
Stepper 5
(off-axis)
Stepper 6
(pivot)
Auxilliary
Switching

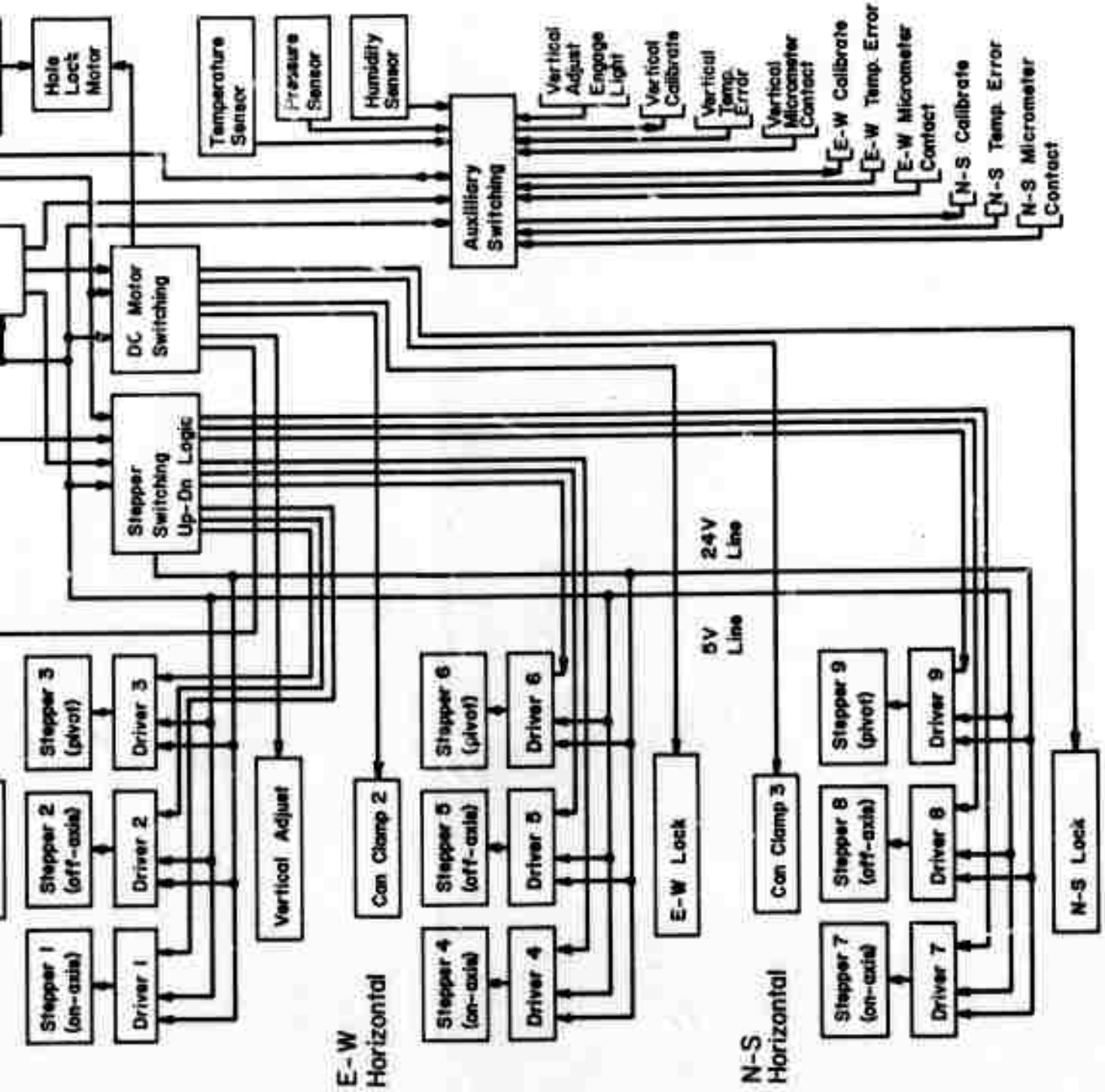
Hole Lock Motor
Temperature Sensor
Pressure Sensor
Humidity Sensor
Vertical Adjust Engage Light
Vertical Calibrate
Vertical Temp. Error
Vertical Micrometer Contact
E-W Calibrate
E-W Temp. Error
E-W Micrometer Contact
N-S Calibrate
N-S Temp. Error
N-S Micrometer Contact
Auxiliary Switching
DC Motor Switching
Stepper Switching Up-On Logic
24V Line
5V Line
Stepper 1 (on-axis)
Stepper 2 (off-axis)
Stepper 3 (pivot)
Driver 1
Driver 2
Driver 3
Vertical Adjust
Can Clamp 2
Stepper 4 (on-axis)
Stepper 5 (off-axis)
Stepper 6 (pivot)
Driver 4
Driver 5
Driver 6
E-W Lock
E-W Horizontal
Can Clamp 3
Stepper 7 (on-axis)
Stepper 8 (off-axis)
Stepper 9 (pivot)
Driver 7
Driver 8
Driver 9
N-S Lock
N-S Horizontal

Fig. II-3

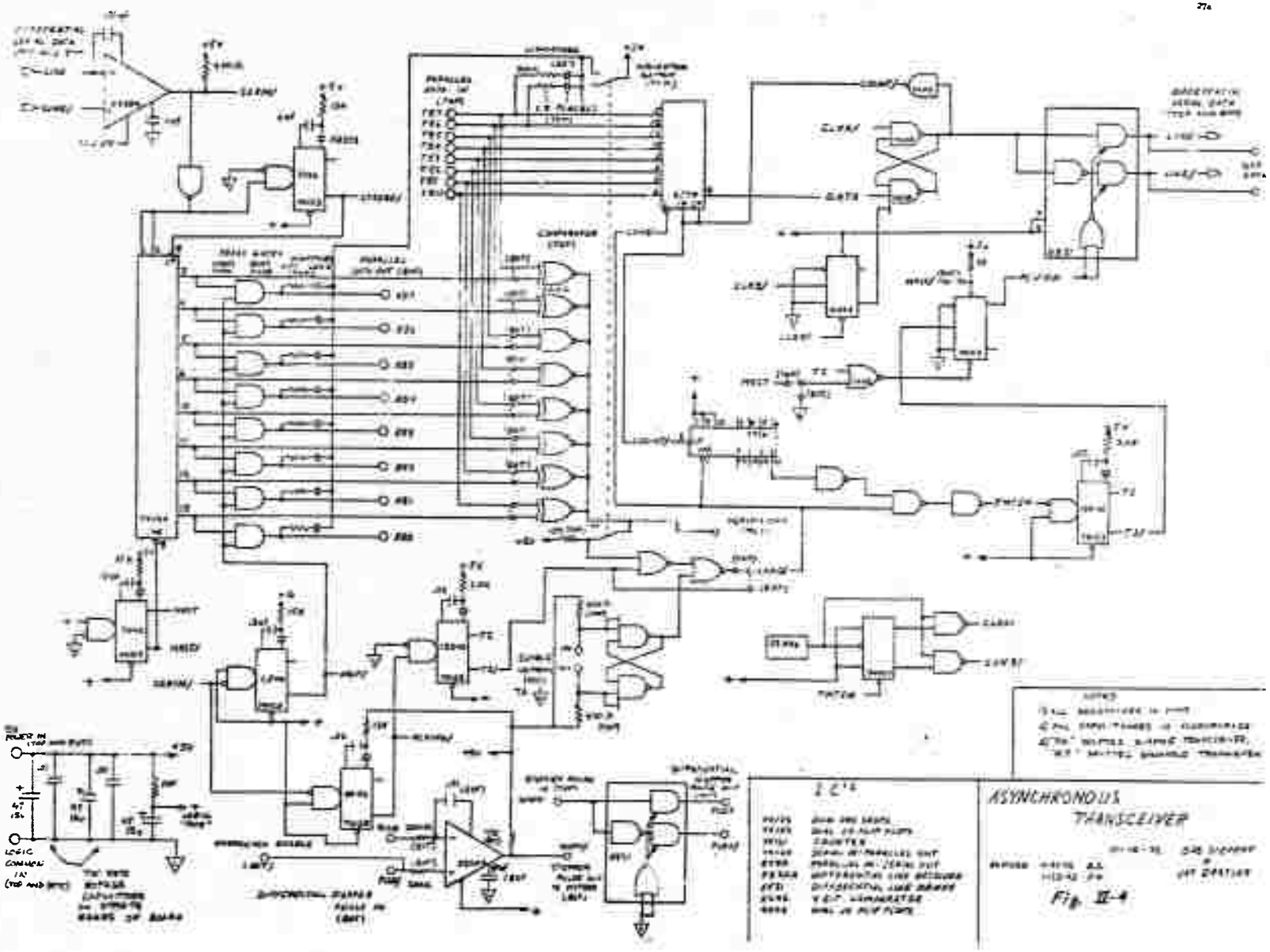

Fig. II-4

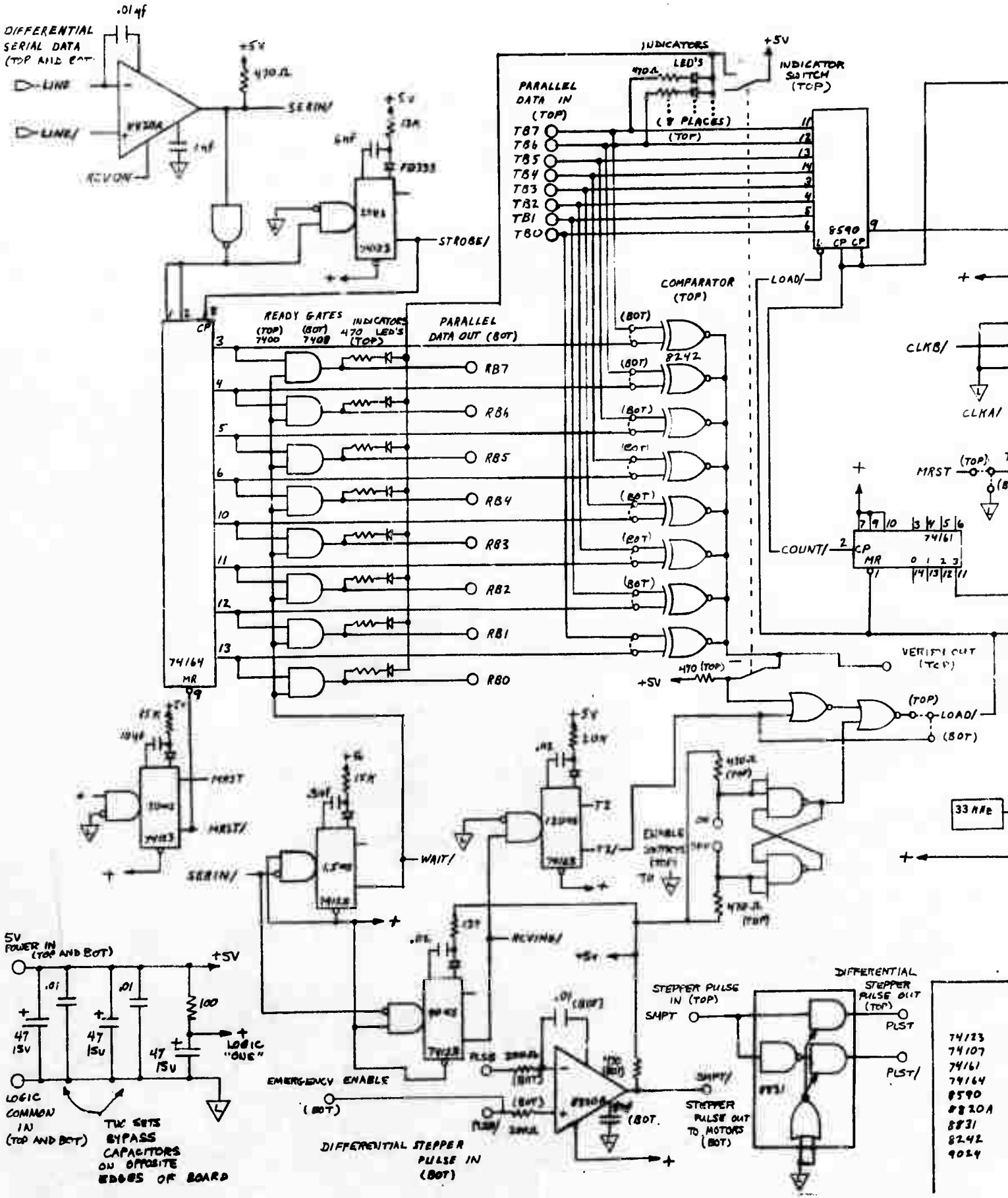
DIFFERENTIAL SERIAL DATA (TOP AND BOT)
LINE
LINE/
RCVDAT
RCVDAT/
SERIN/
STROBE/
PARALLEL DATA IN (TOP)
INDICATORS
LED'S
INDICATOR SWITCH (TOP)
(8 PLACES)
TB7
TB6
TB5
TB4
TB3
TB2
TB1
TB0
8590
LOAD/
COMPARATOR (TOP)
READY GATES (TOP) 7400 (BOT) 7408
INDICATORS 470 LED'S (TOP)
PARALLEL DATA OUT (BOT)
RB7
RB6
RB5
RB4
RB3
RB2
RB1
RB0
74/64
MR
8242
CLKB/
CLKA/
MRST
(TOP)
COUNT/
74161
VERIFY OUT (TOP)
LOAD/
(BOT)
MRST/
WAIT/
T2
T2/
ENABLE SWITCHES (TOP)
RCVINH/
PULSE
EMERGENCY ENABLE
(BOT)
DIFFERENTIAL STEPPER PULSE IN (BOT)
STEPPER PULSE IN (TOP)
SMPT
SMPT/
STEPPER PULSE OUT TO MOTORS (BOT)
DIFFERENTIAL STEPPER PULSE OUT (TOP)
PLST
PLST/
8831
5V POWER IN (TOP AND BOT)
+5V
LOGIC "ONE"
LOGIC COMMON IN (TOP AND BOT)
TWO SETS BYPASS CAPACITORS ON OPPOSITE EDGES OF BOARD
33 MHz
74/23
74/07
74/61
74/64
8590
8820A
8831
8242
9024

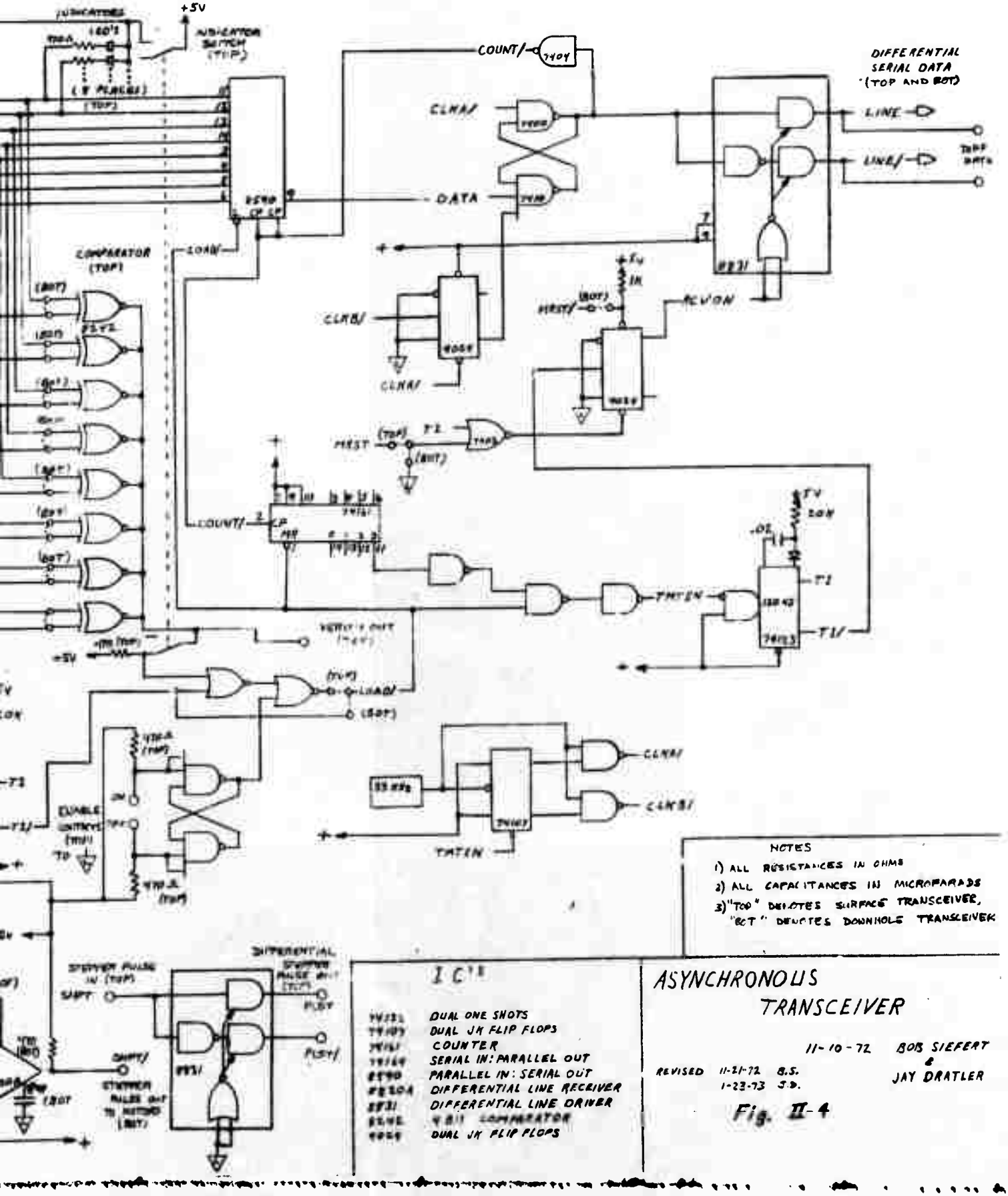
+5V
COUNT/
DIFFERENTIAL SERIAL DATA (TOP AND BOT)
LINE
LINE/
CLKA/
DATA
COMPARATOR (TOP)
LOAD/
CLKB/
RESET/
ACTION
TMTEN
T2
T2/
T1/
CLKA/
CLKB/
TMTEN
NOTES
1) ALL RESISTANCES IN OHMS
2) ALL CAPACITANCES IN MICROFARADS
3) "TOP" DENOTES SURFACE TRANSCEIVER, "BOT" DENOTES DOWNHOLE TRANSCEIVER
IC'S
DUAL ONE SHOTS
DUAL JK FLIP FLOPS
COUNTER
SERIAL IN: PARALLEL OUT
PARALLEL IN: SERIAL OUT
DIFFERENTIAL LINE RECEIVER
DIFFERENTIAL LINE DRIVER
DUAL JK FLIP FLOPS
ASYNCHRONOUS TRANSCEIVER
11-10-72 BOB SIEFERT & JAY DRATLER
REVISED 11-21-72 B.S.
1-23-73 J.D.
Fig. II-4

serve indicator lights which show when any of the leveling micrometers for a given instrument is in contact with the vacuum enclosure or when the zero adjustment coupling for the vertical accelerometer is engaged.

Finally, for relative frequency calibration, selection of one of the calibration channels places a voltage from the surface on the forcing button (Plink stopper) of a given instrument, thus producing an electrostatic force on the inertial element. These channels can be used for sine wave or pseudo random calibration as described in the DIAX publication "Calibration of Broadband Accelerometers with Random Telegraph Signals".

The heart of the sonde controller is an eight bit asynchronous digital transceiver which relays information about the control or switching function to be performed from the surface to the sonde. Figure II-4 shows a schematic diagram of the transceiver circuit, which is used at both ends of the cable. Coded information from switches on the control panel is fed in parallel to the upper transmitter, where a 33 kHz clock oscillator controls the serial transmission to the bottom. The 8 bits are received asynchronously at the bottom and then automatically re-transmitted to the top for verification. If the information received at the top does not check with that sent originally, the original data are automatically re-transmitted. This re-transmission continues until the data are correct or until the process is manually interrupted. During transmission or re-transmission of data, data outputs at the bottom are disabled, so that no function can be performed until some milliseconds after a verified transmission.

Only in the case of the analog signal switching does the receipt of the 8 bits at the bottom initiate a function. When the analog switching command is received, latching relays driven by the logic circuits are activated. These remain set even when power is removed from the controller. For the active functions, however, something besides the coded data is always necessary to initiate activity. The stepping motors require a pulse train to be sent down a separate wire from the surface, and the DC motors require the application of auxiliary motor power. Both the pulse train and motor power are controlled from the surface. This redundancy is necessary to avoid any possibility of potentially damaging errors due to incorrect data transmission.

Coding, transmission, and initiation of control commands are performed at the sonde controller panel at the surface. This panel uses lighted push-button switches with mechanical interlock for simple error-free operation. The user first selects one of three types of functions - stepping motor control, DC motor control, or analog signal switching. Then he selects the particular function, e.g., "move stepping motor number 1 of the E-W horiziontal up". To transmit the code, he presses a momentary enable switch. When the code is received and verified, indicator lights go on, showing the function to be initiated. Finally, the operator turns on the pulse generator or motor power to begin the operation.

The sonde controller panel contains all the power supplies and switching circuitry for driving the motors and monitoring the analog signals. It

includes a variable rate pulse generator with single-step pushbutton for driving the stepping motors and a presettable 7-digit decimal display for counting the steps. There are also meters to monitor analog signals and the current to the motors.

In addition, several protective features are built into the panel. The mechanical interlock on the switches prevents errors due to an attempt to encode more than one function. Enabling the DC motors, which are used mainly in deployment of the sonde, requires activation of two separate switches more than a foot apart. Analog signals emerging from the sonde are buffered so that equipment in the sonde cannot be damaged by shorts or applied voltages at the surface. There is a limiter on the DC power lines which shuts off motor power when the current rises above a certain level. This prevents the casing clamp motor from stalling during deployment. There is an emergency casing clamp activation unit using the stepping motor pulse lines, which allows the sonde to be released in case of a transceiver failure. Finally, a timer is used to allow lengthy operations (such as initial extension of the micrometer legs, taking about 1 hour) to proceed unattended without damage.

Decoding and switching in the sonde is accomplished by a multiplexer board consisting mainly of TTL 4-to-16 line decoders and relays. It too contains a certain amount of redundancy to prevent operations being performed by mistake.

Power for the sonde controller is derived directly from the mains. One 24 V 4.5 amp unregulated power supply provides current for the stepping

motors and the casing clamp motor. Another unregulated power supply (12 V, 9 amp) provides current for the smaller DC motors, and through two separate hybrid voltage regulators, for the logic circuits at the surface and in the sonde. Since the sonde controller is not designed for unattended operation, there are no backup batteries for these supplies.

All of the circuits in the sonde controller have been designed in detail and preliminary drawings have been made. The panel, power supplies, pulse generator, transceivers, multiplexer board, emergency unlock circuits, stepping motor drivers, and counter and display are of in-house design, while the hybrid regulators are OEM items. Detailed designs of circuits other than the transceiver are not presented here, both to conserve space and to allow for modifications dictated by assembly difficulties and the availability of parts.

Circuit board models of the stepping motor drivers have been built and tested. Breadboard models of two transceivers with verifier have also been built and tested. The models work satisfactorily over 500 feet of tightly-coiled two wire shielded cable with 3.3 μf of capacitative loading at each end. This loading is equivalent in capacity to about 300,000 feet of coaxial cable.

Cable Requirements

Table II-3 lists the cable requirements for both the accelerometer electronics and the sonde controller, assuming the conservative design of Figures II-1 and II-3. The size of the conductors is somewhat flexible, being mainly determined by their resistance. For instance, the sonde controller motor power line must carry up to 1.6 amp, which is the stall current for the casing clamp motor. With two 500 ft long conductors of #10 AWG wire, which has a resistance of about 1Ω per thousand feet, 1.6 volts are dropped across the line. Use of finer gauge wire for this power line is possible, but would result in further loss of motor power.

As mentioned above, the number of coaxial elements in the cable may be substantially reduced if the references and/or signals from the three instruments are combined. To determine whether this is feasible, tests with a rag line are necessary. Beyond this, however, the desirability of further reductions in cable size becomes increasingly moot. The sonde controller pulse lines can be eliminated, but only at the cost of removing a protective redundancy. Power cables can be combined, but this involves increased risk of crosstalk and requires complex switching regulators which may radiate interference throughout the sonde.

General Summary

The electronics for the DIAX three axis borehole accelerometer consists of two systems, one for continuous operation of the instruments, the other for control of the sonde. The accelerometer system has been designed using a maximum of commercial equipment, only the temperature controllers having been designed in-house. The drive oscillator, transformer, preamplifier and lock-in amplifier are drawn from the best available OEM items.

The sonde controller is entirely of in-house design, as befits its specialized purpose. Drawings of all circuitry have been made, and the most critical circuits have been built and tested. The system controls the deployment, setup, calibration, and monitoring of the three accelerometers using four control lines, four power conductors, and one coaxial line.

A most conservative attitude has been applied in this initial design. Emphasis has been placed on reliability, foolproofing, and ease of operation, and a conscious attempt has been made to insure that the first DIAX borehole instruments will work as well as their laboratory ancestors.

Concurrent with the construction of the initial borehole system, design work on a miniature lock-in amplifier for use in the sonde is proceeding. If this design proves to have sufficiently low noise and drift, the commercial PAR 120 lock-in amplifiers will be eliminated. Each instrument will use its own DIAX-designed downhole lock-in amplifier, and data from

the three accelerometers will be digitized with a commercial A to D converter module. Transmission of digitized data to the surface will be accomplished by the 8 bit transceiver already designed as part of the sonde controller system. The key to such a system is the miniature lock-in amplifier. Once a prototype has been evaluated in terms of noise and drift, the conservative system design above will be abandoned in favor of a more advanced downhole electronics system. Such a downhole system will result in considerable reduction in cable requirements and has the advantages that the output is intrinsically digital and the critical circuits are inaccessible and in a stable temperature environment.

Table II-1: Commercial Components Used in DIAX Transducer Subsystems

Item	Supplier	Model	Pertinent Specifications
Drive oscillator	Arvee Engineering Co., Torrance, Ca.	OS-101	Amplitude stability .01%/month and .01%/°C
Drive transformer	Donald C. Harder Co. San Diego, Ca.	94023	Secondaries matched to 1 part in 10^4
Preamplifier	Ithaco Ithaca, N.Y.	144E	Input noise of 5 nV/ $\sqrt{\text{Hz}}$ with 80 pf source
Lock-in Amplifier	Princeton Applied Research Corp., Princeton, N.J.	120	High stability and low cost

Table II-2: Estimated Current Requirements for DIAX Accelerometer Electronics

(per instrument)

Downhole	
+24 Volts to Common	Milliamps
Drive oscillator	25
Preamplifier	20
Precision Thermostat	20
-24 Volts to Common	
Drive oscillator	25
Preamplifier	0
Precision thermostat	100
Total current per axis downhole at 24 V	190 ma
Surface	
Lock-in amplifier ($\pm$30 V to common)	150 ea
Total current at surface at 30 V	300 ma

Table II-3: Cable Requirements for DIAX Three Axis Accelerometer

Number	Type	Gauge	Purpose
3	Coax	RG/174	Preamplifier Signal
3	Coax	RG/174	Reference Signal
1	Coax	RG/174	Analog Signals
2	Power	10 AWG	DC Motor Power
3	Power	10 AWG	Accelerometer Electronics Power
2	Power	10 AWG	Logic Power
4	Controller Signals	18 AWG	Transceiver Signals and Stepping Motor Pulses

III. Noise Tests

Introduction

A survey of commercially available low noise preamplifiers and lock-in amplifiers was conducted to determine which components would be used in the detector circuit (Fig. III-1). The noise properties of amplifiers were reviewed and tests were conducted to select the optimum system. Two preamplifiers, PAR model 112 and Ithaco model 144, and four lock-in amplifiers, PAR models 120, 126, and 128 and Ithaco model 391,were chosen for the tests. Although the PAR 112 demonstrated marginally superior noise performance, the Ithaco 144 was chosen for its small size and hermetically sealed package which made it more suitable for borehole deployment. As all of the lock-in amplifiers proved satisfactory, the PAR 120 was selected for its economy, low drift properties and past performance.

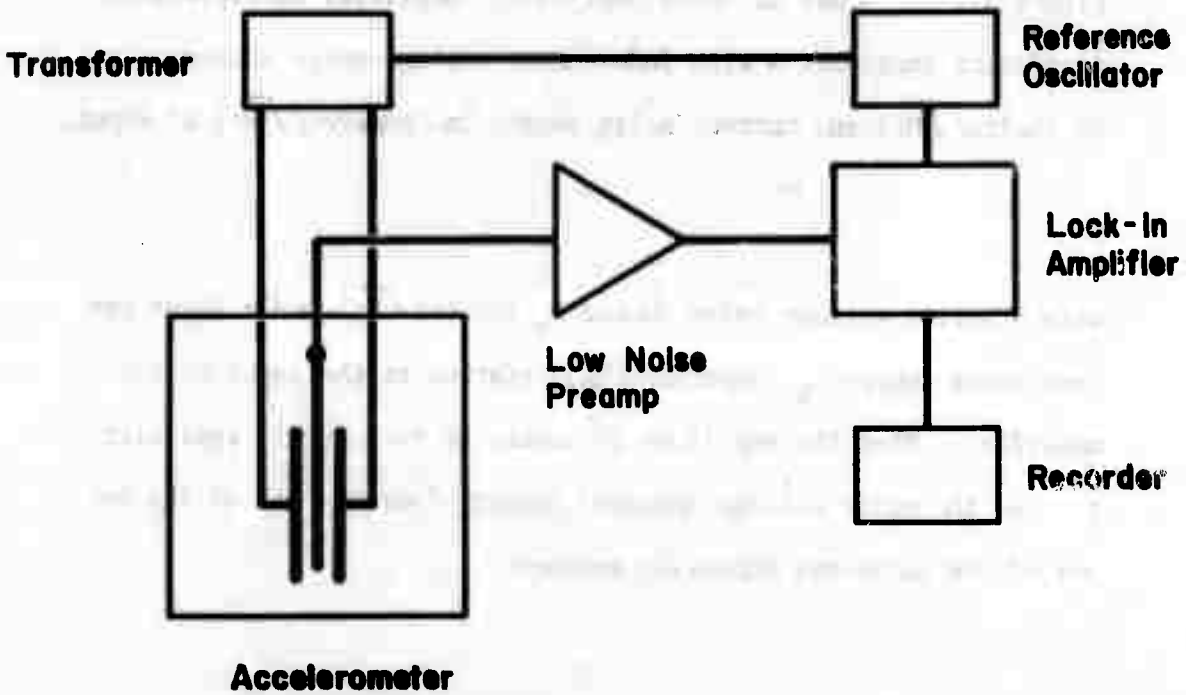

Fig. III-1: Block diagram of detector system for single axis accelerometer

Noise Properties of Amplifiers

A model for the noise generated by an amplifier is shown in Fig. III-2. The amplifier is depicted as a noiseless amplifier A

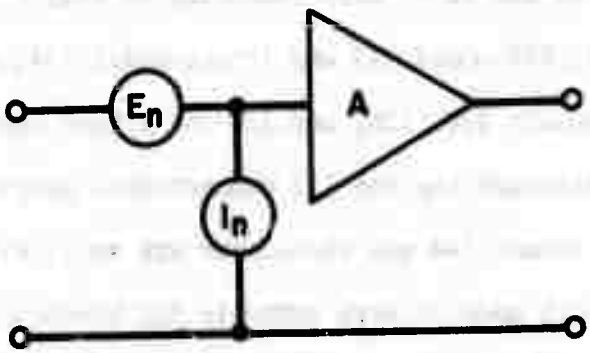

Figure III-2. Model of noisy amplifier. Amplifier is represented as perfect amplifier A with independent voltage noise source En (volts/$\sqrt{Hz}$) and current noise source In (amperes/$\sqrt{Hz}$) at input.

with a series voltage noise source E_n (volts/$\sqrt{Hz}$) and a shunt current noise source I_n (amperes/$\sqrt{Hz}$) referred to the input of the amplifier. When the amplifier is connected to a purely resistive source, the noise voltage spectral density (volts/$\sqrt{Hz}$) at the input of the noiseless amplifier becomes

$$V_{NR} = (4R_s kT + E_n^2 + I_n^2 R_s^2)^{1/2} \quad \text{Volts}/\sqrt{\text{Hz}} \tag{1}$$

assuming the source resistance $R_s << R_{in}$, where R_{in} is the input resistance of the amplifier. Equation 1 assumes that all noise sources are uncorrelated. A more complete description using correlated and uncorrelated noise sources can be found in Ref. 1. Both E_n and I_n are frequency dependent so V_{NR} is a complicated function of source resistance and frequency.

A convenient way to characterize V_{NR} is to use noise figure contours. The spot noise figure $NF(f_o)$ at a fixed frequency is defined as

$$NF(f_o) = 20 \log \left(\frac{4R_s kT + E_n^2(f_o) + I_n^2(f_o) R_s^2}{4R_s kT} \right)^{1/2} \tag{2}$$

$$= 20 \log \frac{V_{NR}(f_o)}{(4R_s kT)^{1/2}}$$

The noise figure represents the ratio of the total noise of the amplifier and source to the thermal noise generated by the source resistance alone. $V_{NR}(f_o)$ can be measured directly in the lab as a function of frequency and source resistance, and since the thermal noise for the resistive source is known, the noise figure can be readily determined. When the noise figure is plotted as a function of

resistance and frequency, the resulting noise figure contours (see Fig. III-3) completely characterize the amplifier noise for resistive sources (at constant temperature).

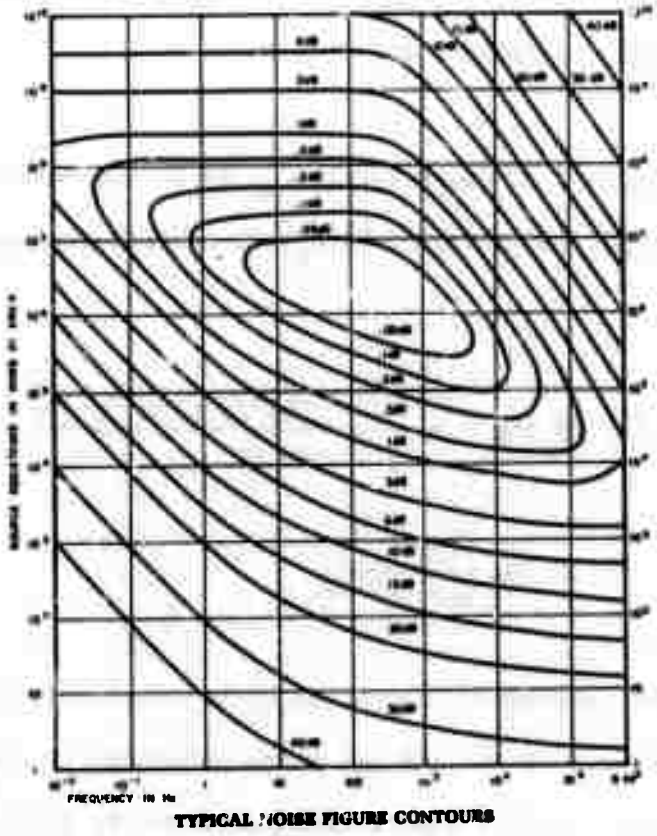

Figure III-3. Example of noise figure contours. Above contours characterize PAR model 113 low noise preamplifier (see PAR Technical Note T-224C-10M-4/71-SP. Reproduced by permission).

For capacitative sources, the situation changes slightly. The noise spectral density at the input of the preamplifier becomes

$$V_{NC} = (E_n^2 + I_n^2 X_c^2)^{1/2} \qquad \text{Volts}/\sqrt{\text{Hz}} \tag{3}$$

where $X_c = \frac{1}{2\pi fC}$ is the reactance of the source. It would be possible to plot contours of V_{NC} against frequency and capacitance, but that is really unnecessary since all of the information is contained in the NF contours for resistive sources, assuming no correlations between E_n and I_n. E_n and I_n can be determined for a given frequency by noting that

$$E_n^2 + I_n^2 R_s^2 = 4R_s kT \tag{4}$$

on the 3 db contours. If the intersections of the upper and lower 3 db contours with the line of given frequency are separated by at least an order of magnitude in resistance, then[2]

$$E_n^2 \gg I_n^2 R_s^2 \qquad \text{(lower 3 db contour)}$$

$$E_n^2 \ll I_n^2 R_s^2 \qquad \text{(upper 3 db contour)} \tag{5}$$

Eq. 4 can be solved for E_n and I_n to give

$$E_n = \sqrt{4kT\ R_E} \quad V/\sqrt{Hz} \qquad \text{(lower 3 db contour)}$$

$$I_n = \sqrt{\frac{4kT}{R_I}} \quad Amp/\sqrt{Hz} \qquad \text{(upper 3 db contour)} \tag{6}$$

where R_E (R_I) are the resistances where the lower (upper) 3 db noise figure contours intersect the frequency of interest. V_{NC} can now be calculated for any capacitance at that frequency, assuming no correlation between input noise voltage and noise current.

The spectral density of voltage noise for the more general case of a capacitor and resistor in parallel can be handled equally well with this model. The magnitude of the impedance of the resistor-capacitor circuit (Fig. III-4) is

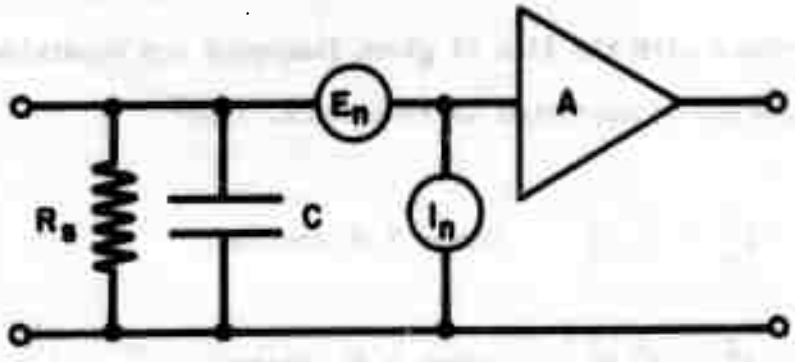

Figure III-4. Model of a noisy amplifier with input shunt resistor and capacitor.

$$| Z_s | = \frac{R_s}{(1 + (\omega R_s C)^2)^{1/2}} \text{ ohms} \qquad (7)$$

The noise voltage at the input of the amplifier becomes

$$V_{NRC} = \left(I_n^2 | Z_s |^2 + E_n^2 + \frac{4R_s kT}{1 + (\omega R_s C)^2} \right)^{1/2} \quad V/\sqrt{Hz} \qquad (8)$$

For frequencies between 10 and 20 kHz, $\omega R_s C >> 1$ ($R_s \sim 10^9$ ohms, $\omega \sim 10^5$ rad/sec, $C \sim 80$ pf for the accelerometer) and Eq. 8 can be approximated by

$$V_{NRC} = \left(\left(\frac{I_n}{\omega C} \right)^2 + (E_n^2) + \frac{4kT}{(\omega C)^2 R_s} \right)^{1/2} \quad V/\sqrt{Hz} \qquad (9)$$

Note the interesting fact that the noise spectral density <u>decreases</u> as the resistance <u>increases</u>. Equation 9 is based on the assumption that the input impedance of the preamplifier is so large that it does not load the circuit.

Noise Tests

Two series of tests were conducted to select the optimum detection system. First, two low noise preamplifiers, the PAR model 112 and Ithaco model 144, were tested to determine which had the lower noise. Then the entire detection system, including the chosen preamplifier and various lock-in amplifiers, was tested.

A block diagram of the apparatus used in the first series of tests is shown in Fig. III-5. A source capacitance of 80 pf, simulating the accelerometer, was connected to the input of the low noise preamplifier being tested. To obtain a measurable signal, the output of the first preamplifier was amplified by the other. Because the noise figures of the two preamplifiers were comparable and both had gains of 100, the

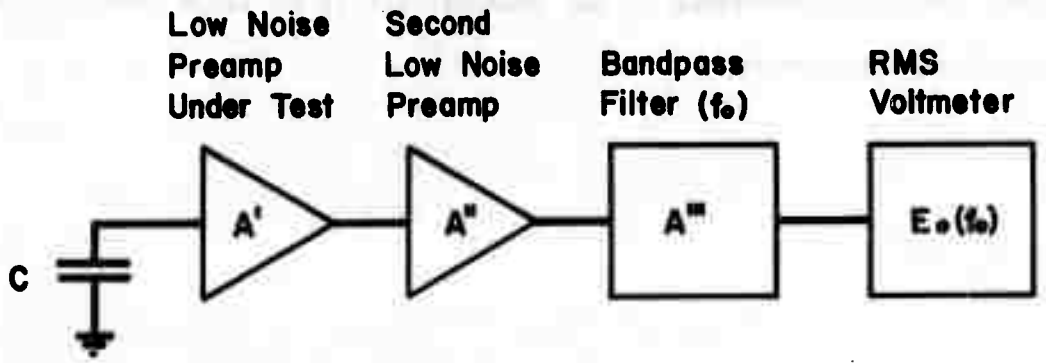

Figure III-5: Block diagram of apparatus for preamplifier noise tests. Two preamplifiers were cascaded to obtain a measurable signal. Switching order of two preamplifiers allowed relative measure of noise levels to be made.

noise introduced by the second preamplifier relative to the input of the first was down by a factor of 100 in amplitude and could be neglected.

The output of the second preamplifier was filtered using a PAR model 210 tuned amplifier and the RMS noise voltage was measured with a Hickok model 3310 true RMS digital voltmeter. The filter had a gain of 10 and bandwidth

$$B = \frac{\pi}{2} \frac{f_o}{Q} \tag{10}$$

where f_o was the center frequency of the filter. The bandwidth of the filter was calculated from the transfer function supplied by PAR. All of the tests were conducted using Q = 100 to obtain the narrowest possible filter ($B/f_o = 1.57 \times 10^{-2}$).

The RMS voltage E_o (f_o) at the output of the filter was converted to amplitude spectral density relative to the first preamplifier input from the known gain and bandwidth of the system.[3] The gain of each preamplifier was 100 and the filter had a gain of 10. For each frequency f_o the bandwidth B of the filter was calculated from Eq. 10. The bandwidth of the system was essentially the bandwidth of the filter because the preamplifiers had bandwidths in excess of 200 kHz. Thus, the noise amplitude spectral density of the first preamplifier relative to its input was calculated from the formula

$$V_{NC}(f_o) = \frac{E_o(f_o)}{A' A'' A''' \sqrt{B}} = \frac{E_o(f_o)}{10^5 \sqrt{B}} \tag{11}$$

where A', A'', A''' were the gains of the various devices in Fig. III-5. Eq. 11 assumes that V_{NC} (f_o) is constant over the narrow bandwidth B. The calculated values of V_{NC} (f_o) were then plotted as a function of f_o. By switching the order of the two preamplifiers, the spectral densities of each were measured, and a quantitative measure of relative performance was obtained.

The data are shown in Fig. III-6. The noise spectral density has

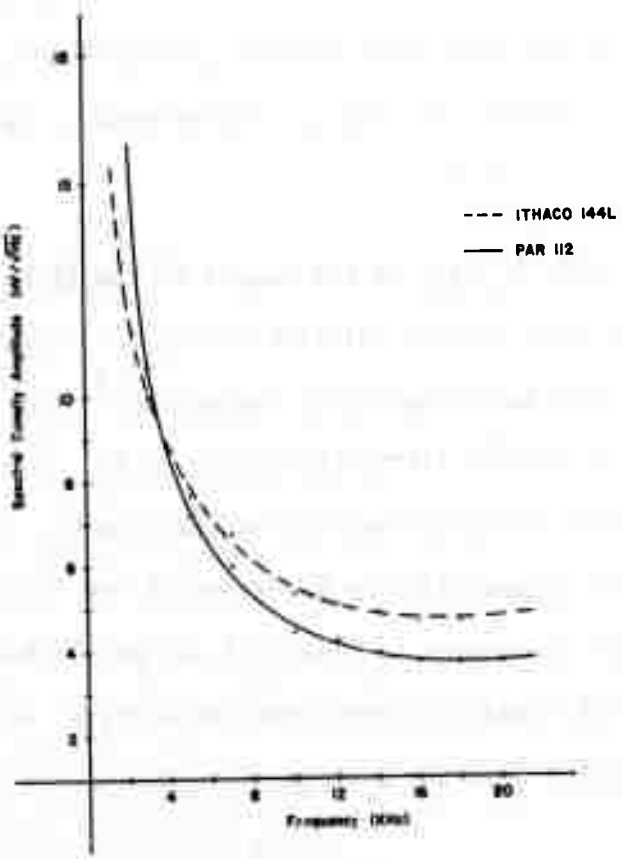

Fig. III-6. Measured input noise as function of frequency for PAR 112 and Ithaco 144 preamplifiers with 80 pf source capacitance. Note broad minimum in noise spectrum near 16 kHz and sharp rise below 4 kHz.

a broad minimum near 16 kHz and rises sharply below 4 kHz. Above 4 kHz the PAR 112 shows a slightly lower noise level. The minimum noise amplitude spectral density for the Ithaco 144 is near 5 nV/$\sqrt{\text{Hz}}$, while for the PAR 112, it is closer to 4 nV/$\sqrt{\text{Hz}}$. If no other requirements existed, the PAR 112 would be the better commercially available preamplifier for use in the detector circuit. However, the PAR 112 was too large and improperly packaged for borehole use. Since it displayed only a marginal noise superiority, the Ithaco 144 was chosen. In subsequent tests of the entire system, the Ithaco 144 was used.

The second series of noise tests was designed to evaluate the performance of various commercial lock-in amplifiers in the accelerometer detector system, and to determine what fraction of the noise was generated by the preamplifier front end. The Ithaco 144 with a source capacitance of 80 pf was connected to the lock-in amplifier as shown in Fig. III-7.

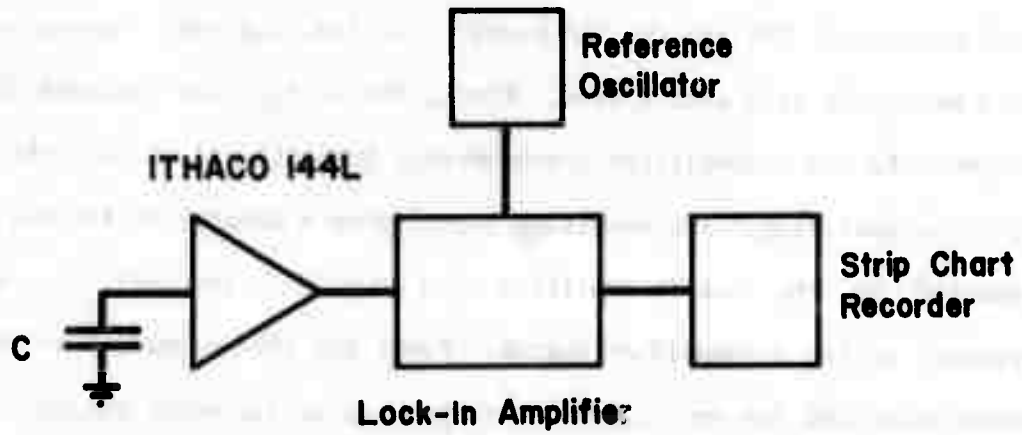

Figure III-7. Block diagram of apparatus for tests of detector system. Entire circuit was grounded at only one point to eliminate ground loops. Ithaco 144 preamplifier was tested with Ithaco 391 and PAR 120, 126, and 128 lock-in amplifiers.

The noise voltage at the output of the Ithaco 144 was detected by the lock-in amplifier relative to an externally generated reference signal at frequency f_o. The output of the lock-in amplifier was recorded on a Hewlett-Packard model 680 strip chart recorder. The RMS value of the output voltage was determined visually from the chart records and converted to an amplitude spectral density relative to the input of the Ithaco 144 by the following formula:

$$V_{NC}(f_o) = \frac{V_{RMS}(f_o)}{A' A_{LIA} \sqrt{B_{LIA}}} \tag{12}$$

where $V_{RMS}(f_o)$ was the RMS voltage estimated from the strip chart record, $A' = 100$ was the gain of the Ithaco 144, A_{LIA} was the gain of the lock-in amplifier, and B_{LIA} was the bandwidth of the lock-in amplifier.

These tests were performed using four commercial lock-in amplifiers, the Ithaco model 391 and the PAR models 120, 126, and 128. Two measurements were made with each system. First, the voltage was recorded with the power to the preamplifier disconnected, but with all of the other apparatus operating. The resulting signal gave a measure of the noise generated by the lock-in amplifier when coupled to the small source impedance of the preamplifier output. Power was then connected to the preamplifier and the new signal, corresponding to the noise voltage of the entire circuit, was recorded. The data taken at $f_o = 16$ kHz are shown in Table I.

TABLE I

RMS noise voltage and noise amplitude spectral density (from Eq. 12) relative to input of Ithaco 144. Tests were performed with Ithaco model 391 and PAR models 120, 126, and 128 lock-in amplifiers.

Reference Frequency f_o = 16 kHz

Ithaco 144 input capacitance C = 80 pf

Lock-in Amplifier	RMS Noise Voltage in nV (144 on)	Amplitude Spectral Density in nV/$\sqrt{Hz}$
Ithaco 391	2.3	7.3
PAR 120	2.6	5.2
PAR 126	3.3	6.6
PAR 128	2.2	6.2

Column 2 of the Table shows the RMS voltages referred to the preamplifier input for the various lock-in amplifiers, with the Ithaco 144 turned on. The output signal with the preamplifier turned off was discernible on the strip chart record but was too small for its RMS value to be estimated with certainty. However, for all the lock-in amplifiers tested, the peak-to-peak noise voltage with the preamplifier on was roughly 100 times larger than that when the preamplifier was off. This result implied that each lock-in amplifier contributed approximately 1% of the noise referred to the preamplifier input. Thus, all of the lock-in amplifiers tested were sufficiently quiet to be used in the accelerometer electronics. The PAR 120 was chosen because of its substantially lower cost, low drift properties, and simple design. It had also been used successfully with the prototype accelerometers.

The amplitude spectral densities calculated from Eq. 12 are shown in column 3 of Table I. The data agree well with the values obtained for the Ithaco 144 from the first series of tests (Fig. III-6). This agreement reaffirms the fact that the lock-in amplifiers add very little noise to the detector circuit.

Errors in the visual estimation of the RMS noise voltages from the strip chart records caused the calculated spectral densities for the different lock-in amplifiers in Table I to differ slightly. They also caused the average amplitude spectral density for the Ithaco 144 from the second series of tests to appear slightly higher than that from the first series. These discrepancies are not significant.

Conclusions

Noise tests of the PAR 112 and Ithaco 144 low noise preamplifiers showed a slight superiority of the PAR 112 in the frequency range 4 - 20 kHz. However, the Ithaco 144 was chosen for the detector circuit on the basis of its small size and sealed package. Further tests with the PAR models 120, 126 and 128 and the Ithaco model 391 lock-in amplifiers indicated that the input noise of these devices referred to the preamplifier input was negligible compared to the noise of the preamplifier itself. Thus, each of the lock-in amplifiers tested had sufficiently low noise for use in the detector system. The PAR 120 was selected for its simplicity, economy, low drift properties, and past performance. The final choices of commercial equipment were the Ithaco 144 low noise preamplifier and PAR 120 lock-in amplifier.

Inquiries made with the preamplifier manufacturer confirmed that a further reduction in front end noise could be had by careful selection of input transistors. With this improvement, the borehole detection system is expected to equal or exceed the performance of the laboratory prototype.

References

1. Hans, H.A. Representation of Noise in Linear Twoports, Proceedings of the IRE, 48, 69-74, 1960.
2. Letzter, Seymour G., Utilizing Noise Figure Contours With Capacitive Sources, PAR Technical Notes TN - 105.
3. Chandler, Donald F., Measuring Noise Spectra with Variable Electronic Filters, Ithaco Applications Notes, IAN - 102.
4. Vander Zeil, A. Thermal Noise in Field-Effect Transistors, Proceedings of the IRE, 50, 1808 - 1812, 1962.
5. Letzter, S. and Webster, N., Noise in Amplifiers, PAR Technical Notes, T - 243. Reprinted from IEEE Spectrum, August 1970, p. 67-75.
6. Princeton Applied Research Corp., How to Use Noise Figure Contours, Technical Notes, T-266 - 20M - 11/69 - MB.